NTNU – Trondheim
Norwegian University of
Science and Technology

Aluminizing of plain carbon steel

Effect of temperature on coating and alloy
phase morphology at constant holding time

Maureen Bangukira Isiko

Light Metals Production
Submission date: July 2012
Supervisor: Ragnhild Aune, IMTE
Co-supervisor: Shahid Akhtar, Hydro Aluminium

Norwegian University of Science and Technology
Department of Materials Science and Engineering

TMT4905 - Materials Technology, Master Thesis

Spring 2012

Aluminizing Of Plain Carbon Steel – Effect of temperature on coating and alloy phase morphology at constant holding time

Maureen Bangukira Isiko

Supervisor: Prof Ragnhild Aune

Co-supervisor: Dr. Shahid Akhtar

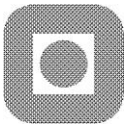

Department of Materials Science and Engineering

Norwegian University of Science and Technology

NTNU

Acknowledgement

I would like to extend my sincere appreciation to both of my supervisors, Prof. Ragnhild Aune at NTNU and Dr. Shahid Akhtar at Hydro for both academic and moral support throughout the course of the thesis.

In the same way I would like to thank Morten Peder Raanes for the help during EPMA analysis, Erlend for training on the use of the micro hardness tester. I wish to thank Delphine Leroy for providing some apparatus that were needed for the coating process. All your efforts were appreciated very much.

Maureen Bangukira Isiko

Abstract

Aluminized steel possesses excellent physical, chemical and mechanical properties as compared to plain carbon steel. This type of steel has found application in high temperature, oxidizing and corrosive environments. In addition, aluminized steel is more cost effective than stainless steels. The objective of the current study is to study effect of temperature on the thicknesses and phase morphology of the coating and intermetallic layer that is formed during hot-dip aluminizing of steel at a constant immersion time of 30 minutes.

1040 steel substrates were aluminized by hot-dipping procedure in pure aluminium and in three different Al-Si alloy melts of varying composition. Hot-dipping was done at three different temperatures mainly at 933, 973 and 1023 K. The steel specimens were held in the melts for 30 minutes after which they were withdrawn from the molten aluminium and allowed to cool to room temperature. The coated samples were then sectioned for metallographic sample preparation. The samples were characterized for thickness of the coating and intermetallic phase thickness and phase composition of both the coating and intermetallic layers. The samples were analyzed by optical light microscope, SEM, EPMA, XRD and micro hardness.

The results show that a greater thickness of the coating and intermetallic layer is obtained with increase in immersion temperature. Two different alloy phases are present in samples hot dipped in pure aluminium while three phases are present in the steel samples hot dipped in the three Al-Si alloy melts. The intermetallic layers have higher vickers hardness values than the coating layer and steel substrate and are more brittle.

List of tables

List of figures

Contents

List of abbreviations and symbols

Symbols	**Meaning**
Al	Aluminium
Si	Silicon
EPMA	Electron probe micro-analyzer
SEM	Scanning electron microscope
HV	Vickers hardness

1. Introduction

Steel is the most versatile structural material in use today and it has been the case for several years from the time of its economical processing by the Bessemer process in the 1850s [1].

Steel exhibits several desirable physical properties such as high strength, elasticity, ductility, toughness, and in addition it is easy to process which makes it the choice of material for numerous structural applications. Despite of the many excellent properties exhibited by steel, there are some undesirable properties like low fatigue strength, susceptibility to brittle fracture and buckling, low corrosion resistance in addition to low strength at high temperatures especially for low carbon steel. As a result of these short comings there are costs associated with maintenance by continuous painting and fire proofing in some cases [2].

Several properties of steel can be enhanced by alloying with one or more alloying elements like sulphur, manganese and phosphorus among others. Such properties include hardness, lowering melting point, strength, corrosion resistance, electrical resistivity, appearance, and castability among others [2].

The surface of materials is the only part that has to co-exist with the external environment, however, majority of engineering failures originate from the surface which then results in the components failures such as fatigue, wear, corrosion and oxidation [2]. To further improve these surface properties various surface modifications can be done through different techniques through which a suitable coating material is deposited onto the steel surface. For steel, surface modifications may include aluminizing, tinning, nitriding and galvanizing among others [3].

2. Literature review

Aluminizing

Aluminizing is a process through which the surface of a metallic component is coated with a layer of aluminum. Steel and its alloys are the most common metals that are aluminized for commercial applications [24].Aluminized steel has good formability and it can be used to make parts containing simple bends with extreme deep drawing requirements. It also has good heat reflectivity and when exposed to temperatures below 700K, aluminized steel can reflect up to 80% of the radiant heat that impinges upon it.

Aluminizing plain carbon steel or steel alloys increases their resistance to oxidation at high temperatures (773-1073K) and also increases the corrosion-resistance of steel in hydrocarbons and sulphurous atmospheres [24].

There are several techniques that have been used to obtain a layer of aluminium over a steel surface on a commercial scale. These include; electrolytic coating, cladding, pack, gas, spray (metalizing) and hot-dip aluminizing. A brief description of the different aluminizing processes is given below.

Electrolytic Coating

In this process electrolytes comprising either a mixture of fused salts of aluminum chloride or aluminum dipped in ethyl bromide and benzene are used. The substrate is first thoroughly cleaned, degreased and pickled in HCl solution [24]. However, the rate of deposition of an aluminum layer onto the substrate is very slow and an average coating thickness of only 0.01 mm could be obtained in around 30 minutes.

Cladding

Cladding involves cold-rolling of sheets of steel and aluminum which results in the formation of a metallic bond between the two sheets, hence bimetallic strip or sheets are obtained [24]. The thickness of the cladding is usually between 2% and 5% of the total sheet or plate thickness, and

since the cladding is usually a softer and lower strength alloy, the presence of the cladding can lower the fatigue strength and abrasion resistance of the product [24]. In the case of thick plate where substantial amounts of material may be removed from one side by machining so that the cladding becomes a larger fraction of the total thickness, the decrease in strength of the product may be substantial [25].

Vacuum Aluminizing

An aluminizing coating is obtained by first vaporizing the pure aluminum or aluminium alloy and then condensing it onto the steel substrate. A vacuum chamber pressure of 10^{-3} - 10^{-5} mm of Hg is required and electron beam devices are used to melt the aluminum and raise its temperature up to about 1673K. In addition the substrate must be heated up to 448-643K. This process gives a good coating adherence. The coating thickness in this case is of the order of 0.1 μm [25].

Spray Aluminizing (Metallizing)

An aluminum coating of specific thickness is sprayed onto a pre-cleaned steel surface [24]. The process involves melting and spraying molten metal by a jet of compressed air between 25-60 psi with special metallizers. The bond obtained is of low strength, although the surface adherence can be improved by increasing the surface roughness of the substrate. Annealing to temperatures 1123-1523K for a sufficient amount of time may be done to increase the bond strength.

Gas Aluminizing

During gas-aluminizing, the steel substrate is impregnated with aluminum using a gaseous phase of aluminum chloride [25]. This is carried out in a retort, and the composition of the gas mixture is given as 45% Al, 45% Al_2O_3 and 10% $AlCl_3$.

The mixture in the retort is heated to 873K and the substrate is positioned at the opposite end of the retort where it is heated to 1173-1273K. The impregnation of steel with aluminium proceeds according to the following reaction: $AlCl_3\,(g) + Fe\,(s) \longrightarrow FeCl_3\,(s) + Al(s)$

This method is not commonly used for industrial aluminizing of steel because it is a complex and energy intensive process [24].

Pack Aluminizing

The substrate is first cleaned then packed in air-tight retorts with an aluminizing mixture, which consists of aluminum or ferro-aluminum dust/ powder and heated to the aluminizing temperature for up to 30 hrs. This method is expensive and time-consuming and is only recommended for articles of intricate shapes. Typical applications of pack-aluminizing are nickel-based alloys used in gas turbines. However, steel can also be pack-aluminized to improve its high temperature oxidation resistance [24].

Comparison of aluminizing methods

Although several methods that can be used to deposit a layer of aluminium on to steel surfaces, however, hot-dip aluminizing was chosen as the most feasible technique according to the study done by V.R Ryabov [8]. In table 1 below a comparison was made of five different methods of aluminizing and the best method was chosen basing on four parameters as shown in the table.

Table 1 Comparison of different aluminizing methods [5]

Process	Thickness of coating (mm)	Coating cost	Relative intermediate	Absence of continuity of coating
Hot-dipping	0.01-0.08	1	2	2
Cladding	0.01-0.13	2	3	1
Galvanic (electrolytic)	0.003-0.05	3	1	3
Spray (metalizing)	0.05-0.50	4	1	4

Rating 1 indicates the best result [5].

According to the table above, hot-dip aluminizing method displays a combination of low operational costs, a relatively good coating continuity and intermediate alloy thickness, making it

the preferred method for commercial aluminizing process of steel. It can also be observed that it yields a lower coating layer thickness which may result in a thinner intermetallic layer which is desirable for a longer life of the protective aluminium layer. This aspect will be further explained in this chapter. Hot-dip aluminizing is a simple technique of coating steel but in some cases it involves extra costs for surface-cleaning, fluxing and after treatments.

2.1 Aluminized steel

Aluminum spontaneously forms a passive aluminum oxide film which is a typical characteristic of aluminum. This film imparts its resistance to major environmental factors influencing corrosion in water and soils [24]. Corrosion due to dissolved gases like CO_2 and erosion corrosion due to high velocity of water are the common factors contributing to corrosion of pipes in a waterside environment. The passive film exhibits higher resistance to all of these factors.

Pure aluminium and aluminium silicon alloys were chosen as coating materials because aluminized steel has shown superior resistance to atmospheric, salt spray and muffler condensate corrosion. Corrosion rates of steel coated with Al, Al-Zn alloy and Zn are shown in table 2[2].

Table 2: Corrosion resistance of aluminized steel

Environment	**Al Type 1-40**	**Zn-Al alloy G50**	**Zn G90**
Muffler condensate annual corrosion rate (mg/cm)	8	16	27
Salt spray(hrs to red rust)	500	1000	200
Industrial annual loss (mg/cm)	0.25	0.98	1.5
Atmospheric-marine (mg/cm)	0.62	1.16	4.5

It is observed from the comparison of steels coated with different metals to undergo corrosion in different kinds of environments and aluminized steel shows the slowest rate of muffler condensate annual corrosion rate, lowest industrial annual loss and atmospheric-marine corrosion rate and on the other hand, it takes the least time to turn to red-dust under the salt spray.

Applications of aluminized steel

There are several areas of application for aluminized steels mainly where high temperature strength, oxidation and corrosion resistance is critical.

One such area is in exhaust pipes which consist of front exhaust pipe connecting the exhaust manifold to the catalytic converter, an intermediate exhaust pipe connecting the catalytic converter to the muffler, and a tailpipe connected to the outlet of the muffler and serving as the exhaust outlet [2].

Figure 1: Aluminized Steel Exhaust System for Mazda RX8 with Stainless Steel Tailpipes

Other applications include water heaters, brooder reflectors, furnaces, dry kiln walls and doors, heat exchangers, home and industrial incinerators and drying ovens plus many others [3].

2.3 Hot Dip aluminizing process

Hot-dip aluminizing is one of the oldest and most widely used processes for depositing a layer of aluminium onto a steel surface. It involves four major steps;

1) Pretreatment: It is done whereby the surface of the substrate is cleaned to remove dusts, grease and rust if present to increase adherence of the coating. It can either be done mechanically by grinding or chemically by pickling in dilute hydrochloric or sulphuric acid **[13]**.

2) Fluxing: Fluxing is done to increase wetting of the substrate by the molten metal during dipping in molten aluminuim. This step also serves for further cleaning by immersing the substrate in a molten salt flux floating on top of the molten bath before immersion into the coating bath.

3) Coating: The substrate is dipped in the molten bath for specific duration of time. The technique used will differ according to the shape and size of substrate that is to be coated.

4) After-treatment: This refers to wiping, air-blasting or rolling of coated steel after withdrawal from coating bath. The objective is to reduce the amount of metal adhering to the sample.

Hot-dip coating process description

For the preheating and fluxing processes, the cleaned substrates are dipped in a fused salt mixture (40% NaCl, 40% KCl, 10% AlF_3, and 10% Na_3AlF_6) for 8 to 15 min at 975K [24]. The steel substrates are in constant motion during the preheating, fluxing and coating processes to remove any trapped air and to flux all surfaces of the part thoroughly.

In some coating processes, the pickling and fluxing operations are eliminated and instead the steel parts are simply blasted with abrasive grit and then immersed into the molten aluminum bath. Unless the process is carefully controlled, this procedure has some of the disadvantages below;

(i) Steel parts heated up to the coating temperature in the molten aluminum produce a thicker alloy layer.

(ii) Dissolving additional iron into the bath.

Controlling the temperature of the molten coating bath is very important because higher coating temperature increases the thickness of the intermetallic layer but does not necessarily increase the thickness of the pure aluminum coating layer.

Industrial aluminizing process

A continuous line of hot-dip aluminizing of strips usually consists of a feeding section, furnace, and delivery section. In the feeding section, incoming strip are uncoiled and fed into the coating line at a pre-set speed under fixed tension. The furnace section consists of the preheating, annealing, cooling and coating furnaces. If chemical cleaning is done, alkaline cleaning and water rinsing tanks are included instead of the preheating furnace [A]. The cooling furnace is connected to the annealing furnace and extends to the coating bath. It is sealed by means of a snout which extends into the molten aluminum bath. In the annealing and cooling furnaces, a dry reducing atmosphere of hydrogen and nitrogen is maintained. The delivery section is equipped to rapidly cool and allow sufficient time for the coating to set before the strips come in contact with the support roll over the coating bath.

The delivery section consists of drive rolls and equipment for looping roller, leveling, coiling and shearing. This section also contains stretch leveling and surface conditioning.

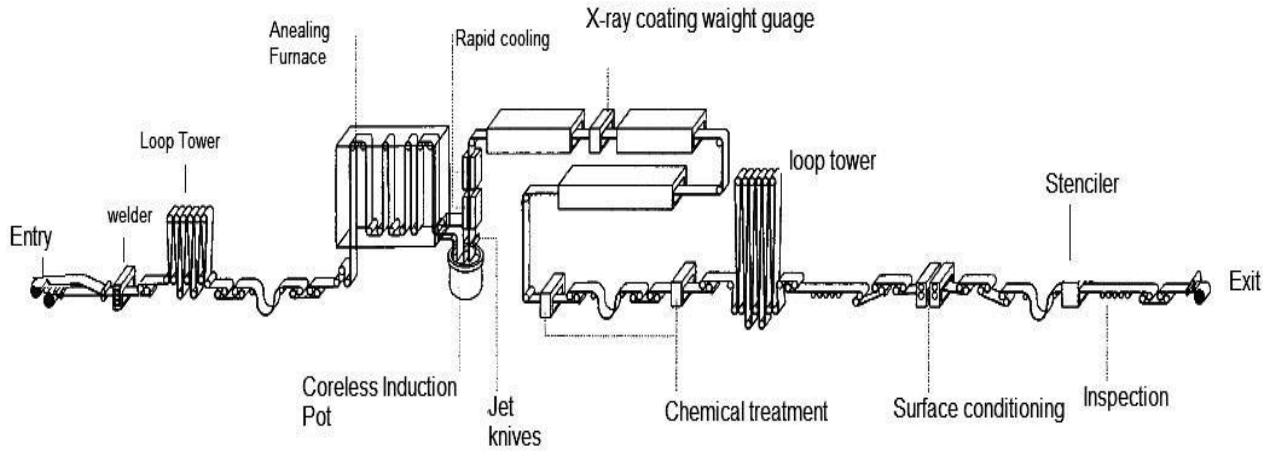

Figure 2: Process diagram of continuous hot-dipping of steel strips [24]

Aluminizing makes steel more corrosion and oxidation resistant even at elevated temperatures up to 1173 K [6]. However, at the coating temperatures which are usually above 923 K, a reaction occurs between molten aluminum and the steel substrate leading to the formation of an intermetallic layer at the interface of the substrate and the coating which is harder and brittle. This may substantially reduce the ductility of steel and hence limiting the purpose of aluminizing as a means of protection for sheet materials that will be subjected to further forming, bending and/or other types of plastic deformation [7].

When a steel substrate is dipped in a pure aluminum melt for a sufficient period of time which may vary from 1 min and above, the intermetallic phase formed in the steel consists almost of only η phase (Fe_2Al_5). This has been attributed to the favorable crystallographic orientation of the η phase by K. Schubert [8] as well as the higher growth rate of this phase. The growth of the alloy layer is commonly represented by the expression below;

$$\sigma^2 = kt$$

Where σ is the thickness of the alloy layer, k is a constant known as the growth rate constant, and t is the holding time. The growth rate constant of the θ phase ($FeAl_3$), as calculated by Eremenko [1] , was $2.1\times10-7$ cm^2/s at 715°C, while the growth rate constant of the η phase, as calculated by Heumann and Dittrich [10] , was $2.2\times10-6$ cm^2/s at 988K. Table 3 gives the standard enthalpy and entropy changes at 298K, and Gibb's free energy changes at 973K accompanying the formation of Fe–Al phases [11].

Table 3: Standard enthalpy, ΔH^0, and entropy changes, ΔS^0 (at 298 K) and Gibb's free energy changes, ΔG (at 973 K) accompanying formation of Fe–Al phases [11]

Phase	ΔH^0	ΔS^0	ΔG
	(K^{-1} mol^{-1})	(kJ mol^{-1})	(kJmol^{-1})
θ-$FeAl_3$	−112.5	95.6	−22.8
η-Fe_2Al_5	−194	166.7	−19.6
ξ-$FeAl_2$	−81.9	73.3	−16.9
α-FeAl	−51.2	51.0	−11.0
Fe_3Al	−57.3	28.0	−4.8

This intermetallic layer advances into the steel substrate by forming a ragged, finger-like front which is mainly composed of Fe_2Al_5, but traces of FeAl and $FeAl_3$ are sometimes reported to be present [12].

Better performance can be achieved during deformation by reducing the intermetallic layer as much as possible and this can be achieved by reducing the immersion time and/ or the aluminizing temperature. An intermetallic layer thickness, about 25% of the total coating exhibits better bending properties but leads to a reduction in useful life of the coating.

A thinner outer coating with thinner intermetallic layer performs also well under tension, but is susceptible to collapsing under pressure. Fe can react with Al under certain conditions to form five different intermetallic compounds which include $FeAl_2$, $FeAl_3$, Fe_2Al_5, FeAl, and Fe_3Al as shown in figure 3 [12].

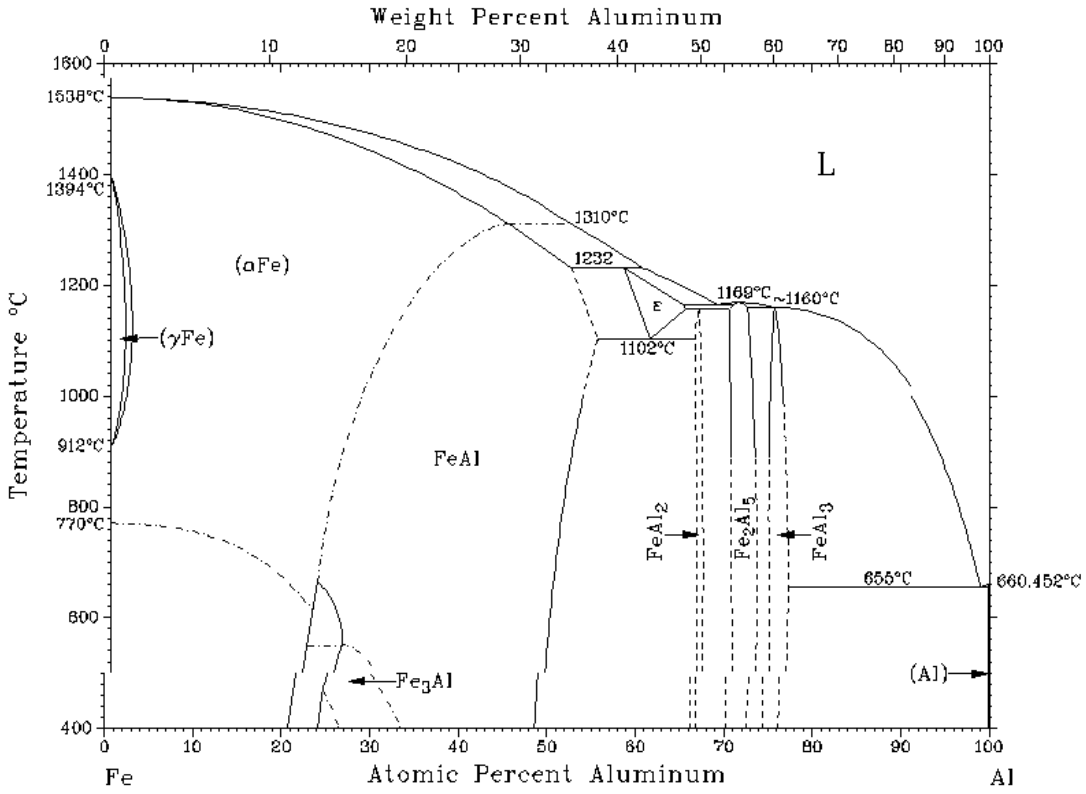

Figure 3: Phase diagram of Fe and Al showing phases formed [12]

The intermetallic compounds like $FeAl_2$, $FeAl_3$, and Fe_2Al_5 which have high aluminium content are brittle and may be problematic [12]. Conversely, Fe_3Al and FeAl with high iron content show good wear resistance, oxidation resistance, corrosion resistance and specific strength properties [14] and they may be used as structural materials. Therefore, the preferential growth of Fe_3Al and FeAl layers could improve the fracture toughness, oxidation resistance and interface strength of aluminized steel. However, in table 3 it can be observed that the intermetallic compounds rich in Al like $FeAl_3$, and Fe_2Al_5 posses much more negative standard enthalpy of formation and gibbs energy changes. They are therefore formed more easily.

The interlayer thickness is mainly affected by the immersion time and the temperature of the bath. A change in the carbon content, composition of the steel substrate and that of the coating bath may also have a marked effect on the growth and morphology of the intermetallic layer [13]. The thickness and morphology of the intermetallic layer may be affected by additions to the molten bath, such as silicon to an aluminum bath. The viscosity of the molten metal and the roughness of the surface being coated inevitably affect the amount of liquid metal that adheres to the substrate while taking it out of the molten bath.

The other factors which may affect the growth of this layer include the speed of withdrawal of the article, the temperature of the metal and the time interval during which the coating layer is molten [13].

Unless a void layer separates the alloy phase from the base metal (steel), the amount of iron in the alloyed coating increases with time as the iron continues to diffuse into the available molten aluminium [24].

The quality of aluminizing is markedly affected by the cleanliness of the surface of substrate. If the surface of the substrate is not well cleaned, the molten aluminium does not wet the surface completely and therefore in areas where there is no wetting, there is no reaction leading to the alloy phase formation. It is worth noting that during hot-dip aluminizing, to obtain a permanent layer of Al coating, a chemical reaction must occur forming the intermetallic layer which on cooling , fuses together the outer coating to the inner steel phase [24].

2.4 Factors that influence the aluminizing process

A number of factors play a critical role in the process of hot dip aluminizing some of which influence the thickness of intermetallic layer, morphology and phase composition while others influence the surface adhesion of the coating.

a. Formation of the intermetallic layer due to the chemical reaction between iron in the steel and aluminium in the coating.

b. The interlayer is affected by the dipping time and aluminizing temperature.

c. The carbon content of the steel substrate may also have a marked effect on the growth rate and morphology of the intermetallic layer [13].

d. The thickness and morphology of the intermetallic layer may be profoundly affected by additions to the molten bath, such as silicon.

e. The viscosity of the molten metal may influence the wetting of the substrate.

f. The roughness of the substrate surface determines the amount of layer of molten metal that adheres to the substrate during withdrawal from molten bath.

g. Other factors are temperature of the metal and the time during which the coating layer is still liquid and free to draw off. During this time, the coating cools and solidifies and the intermetallic layer grows by consuming the outer layer of aluminum completely converting it to an alloy [13].

Effect of silicon

It was reported by Sundqvist and Hogmark [15] that the addition of silicon to an aluminum alloy hampered the growth of the intermetallic phase of Fe_2Al_5 in the hot-dip aluminizing process. The growth kinetics of this phase has been reported to be diffusion controlled and that the rate determining step is the diffusion of Al atoms through the boundary layer Fe_2Al_5 [6] .

Nicholls [16] explained further that silicon has ability to change the diffusion conditions of the Fe_2Al_5 phase and reduces solid state growth. Silicon occupies the structural vacancies in the Fe_2Al_5 phase which allow for Al diffusion to promote the growth of this phase.

Komatsu et al [17] reported that silicon addition to the coating bath accelerates the velocity of iron enrichment in initially iron-free aluminum melts; this iron combines with free Al and forms new phases resulting in decrease in diffusion of Al atoms towards the substrate and consequently decreases the growth of the intermetallic layer. Since the growth rate of binary Fe-Al intermetallic is higher than that of interfacial Fe_x Si_y Al_z alloys, the thickness of the Fe-Al layer is not affected significantly by the temperature.

The thickness of the interlayer rapidly decreases as the silicon content increases to 2.5 at. % (5 wt. %) and no significant further decrease in thickness is observed for Si content beyond 6 % [18] and in addition the apparent ductility of the coating enabling more severe fabrication without peeling[6]. Figure 2 below shows the effect of Si content in Al bath on interlayer thickness [4] .

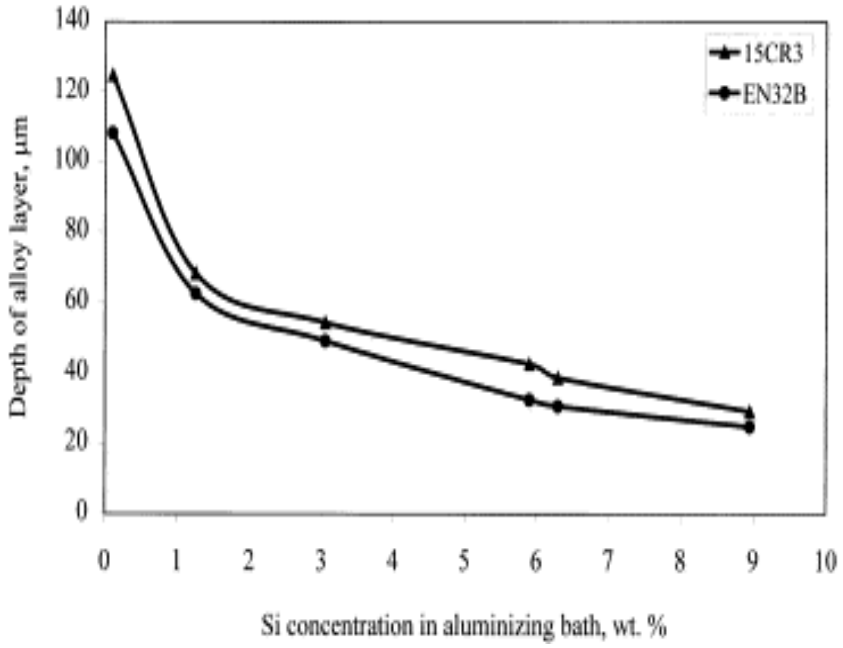

Figure 4: The effect of Si content in Al bath on interlayer thickness [4]

Effect of carbon content

The carbon content of steel substrate has been reported to influence the thickness of the interlayer during hot-dip aluminizing. Studies by Teng-shih shih et al [19] have shown that a lower carbon content of the steel substrate increases the thickness of the intermetallic layer for both short and long dipping times. Two types of steel samples, 1020 and 1040 were compared. Table 4 below shows the thickness of the intermetallic layers of steel samples coated with pure Al. The steel 1020 has both lower carbon content and a higher fraction of ferrite than steel 1040.

Table 4: Effect of carbon content in steel on the interlayer thickness [19]

Time (min)	Thickness ((µm)	Thickness ((µm)
	1020 pure Al	1040 pure Al
3	NA	16-22
10	82-136	45-50
20	91-200	114-136
40	200-318	227-236
60	291-336	264-282

The lower carbon steel 1020 substrate had a larger intermetallic layer thickness than steel 1040 when dipped in the pure Al melt, because more ferrite was available at the interface to react with the Al melt.

The intermetallic layer would advance more quickly into the steel substrate when there was more ferrite located at the tip of the interfacial front. In addition, the reactive phase shows favorable growth into the steel substrate via the ferrite grain boundaries and the finger-like morphology therefore becomes much more apparent as compared to the steel 1040 when dipped in the same pure Al melt.

Figure 5(a) shows the growing front of the interlayer protruding into the ferrite substrate associated with aluminium carbide or carbon trapped in the intermetallic layer.

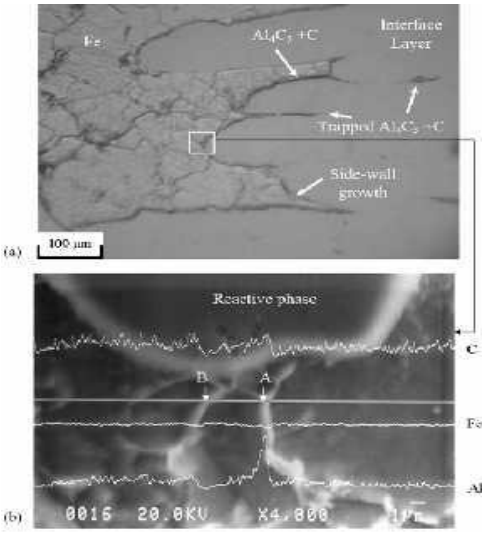

Figure 5: Growing front of the interlayer protruding into the ferrite substrate [19]

The Fe, C and Al concentrations in regions at the tip of the finger like structures were measured by electron probe microscope analyzer and the figure 5(b) shows the phases.

Carbon content was relatively higher at the grain boundaries at points A and B than inside the grain. Al diffuses through the interlayer towards along ferrite boundaries into the grains; it reacts with carbon at grain boundaries forming Al_4C_3 which leads to ferrite diffusion to the boundaries where it then reacts with Al to form the Fe-Al alloy compounds. The reaction steps leading to the formation of Fe_2Al_5 were suggested as follows [19]

$Fe + Al = FeAl$ *(-11.09kJ/mol)*

$FeAl + Al = FeAl_2$ *(-16.99 kJ/mol)*

$FeAl_2 + Al = Fe_2Al_5$ *(-19.64 kJ/mol)*

From the Gibbs energy values for the formation of the alloy phases above, it is evident that the Fe_2Al_5 phase forms easily and it is likely to be the dominant phase.

Effect of dipping time

Teng-Shih Shih et al [19] studied the effect of dipping time on the growth kinetics of the intermetallic layer. Figure 6(a-d) shows the progressive development of the intermetallic layer and the interface between the 1040 steel and the pure Al, for dipping times of 10, 20, 40 and 60 min, respectively. For short dipping times, the thickness of the intermetallic layer varied significantly and the interface was rough and uneven. Some areas displayed a thicker intermetallic layer; however in some locations it was very thin, as shown in figure 6(a).

As the dipping time was increased the interface became more ragged and showed finger-like morphology in figure 6(b). Further increase in the dipping time caused the ragged interface to become smoother, but pores were generated in the intermetallic layer, as shown in figure 6(c).

The interface became bumpy again for longer dipping time like 60 min as seen in figure 6(d). The morphology of the interface between the intermetallic layer and the steel substrate differs depending on the dipping time and is affected by carbon diffusion in the substrate, aluminum diffusion in the intermetallic layer and their interaction.

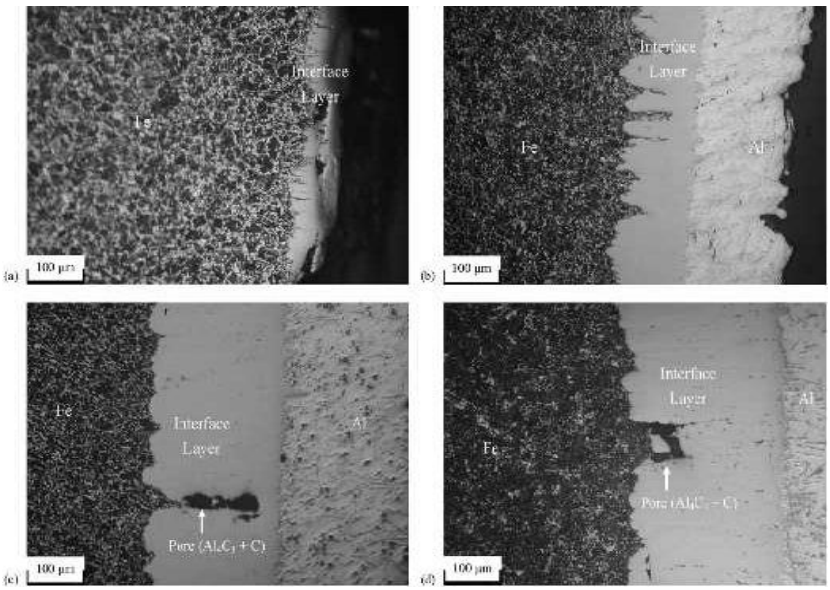

Figure 6: Progressive development of Intermetallic layer and interface between 1040 steel and pure Al after different dipping time periods: (a) 10 min; (b) 20min; (c) 40min; (d) 60 min [19]

Effect of temperature on intermetallic layer

The effect of immersion temperature on the interlayer compounds in hot dip aluminized steel was previously studied by S. Kobayashi [18] for temperatures from 873-1373K and a dipping time of 300s (5 min). It was reported that the thickness of the coating increased with higher coating temperatures. In comparison with the thickness of the two formed layers, the Al layer at the surface grew from 100 to 200µm and the Fe_2Al_5 grows rapidly as temperature was raised from 973 to 1073K beyond which the growth of this phase was saturated. However the interface of the Al and intermetallic alloy phase remained flat. Figure 7 [6] shows the cross sections of specimens with dipping temperatures ranging from 973-1123K.

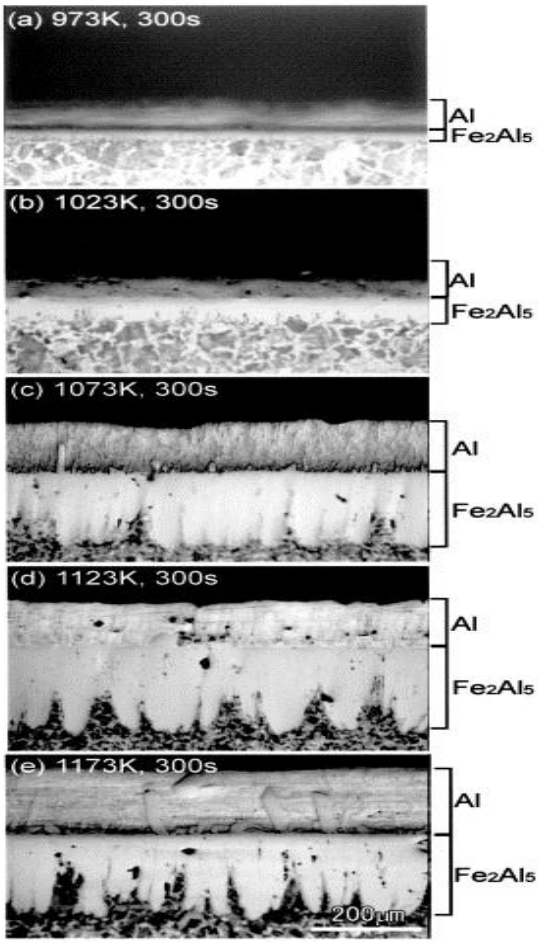

Figure 7: Cross section micrographs of specimens immersed at (a) 973 K, (b) 1023 K, (c) 1073 K, (d) 1123 K and (e) 1173 K for 300 s [6]

Growth kinetics of intermetallic layer

The rate of growth of the interlayer is known to be dependent on a number of factors. The factor that will be focused on is the chemical composition of bath and substrate.

V.N. Yeremenko [1] studied the effects of various impurities present in the molten Al during hot-dip coating on the morphology of the interlayer. It was reported that at immersion temperature of 973-1023K the alloy compound formed initially is $FeAl_3$ followed by Fe_2Al_5 between the steel and the $FeAl_3$ phase [9]. The activation energy for growth of Fe_2Al_5 layer was reported to be 155 $kJmol^{-1}$ between 973-1073K.

It was suggested that formation of phases with high Al content was dependent on diffusion coefficients of Fe into Al [9]. The diffusion coefficient of Fe in Al is 53 x 10^{-4} m^2s^{-1} between 823-923Kwhile the diffusion coefficient for Al into Fe is 1.8 x 10^{-4} m^2s^{-1} between 1003 and 1673K [20].

Elements such as Si, Cu, Mg and Cr have an effect of decreasing the activity coefficient of Al atoms therefore reducing the thickness of the interlayer while Mn,Ni, Pb and Bi increase the activity coefficient of Al atoms and consequently the thickness of the Fe-Al alloy phase[21].

$$\gamma_{Al} = (y_{Al}/y^{\circ}_{Al}) \ldots\ldots\ldots\ldots\ldots\ldots\ldots\ldots\ldots\ldots\ldots (i)$$

$$(y_{Al}/y^{\circ}_{Al}) = \varepsilon^2 Al.C_{Al} + \varepsilon^3 Al\ C.X + \ldots\ldots\ldots\ldots (ii)$$

The first term in equation *(ii)* gives the interatomic interaction parameter between Fe and Al while the second term gives the impurity effect on the interatomic interaction in the Fe-Al-X ternary system.

3. Experimental method

1040 steel substrates with composition (Table 5) were prepared by milling and cutting to remove the external rusty layer and to obtain a relatively smoother surface suitable for coating. The samples dimensions (1.5cm width, 5.0cm length and 0.5cm thickness) were cut from the ingots and holes of 3mm were drilled at one of the ends of each specimen. They were fastened with thin steel wires so that they could hang on a jig above the molten metal bath during hot-dipping experiments.

Table 5: Chemical composition of 1040 steel

Elements	C	Mn	P	S	Fe
Amount (Wt %)	0.37-0.44	0.60-0.90	0.045	0.050	bal

Surface preparation and cleaning

Cleaning of the substrates surface was done by two cleaning processes.

(a) Acid cleaning: The samples were dipped in (5v/v %) sulphuric acid solution for 30 seconds followed by rinsing with water, flushing with ethanol and rapid drying by air blowing. The samples were then placed in glycerol to prevent them from re-oxidation before dipping. Dipping samples in glycerol posed a challenge whereby the glycerol burnt off when the samples were immersed which resulted in sparks. The glycerol layer was burnt in a separate furnace at a temperature of 823K which also served to pre heat the samples for 10 minutes before dipping. Burning off the glycerol however left the acid-cleaned surface of the steel substrate unprotected and this promoted even faster oxidation in some areas and a residual carbon that appeared as a layer of soot on the sample surface.

The surface of the substrate was no longer clean enough and although pre heated, it was not wettable which led to weakly adhered aluminium coating layer at the higher dipping temperatures of 973K and 1023K and completely unattached coating layer at 933K even after the immersion

time of 30 minutes. This procedure was only used with a pure aluminium bath and since it produced an unacceptable result it was not used for the aluminium-silicon alloys.

(b) Grinding with SiC paper: The remaining steel samples were ground with 320 and 500 SiC papers, after which they were rinsed with water and ethanol then dried rapidly using a blow drier. This yielded a smoother and cleaner surface. These were kept in LD-polyethlene bags to prevent them from oxidation by air.

Figure 8: Prepared samples cleaned by grinding before coating

Hot-dip aluminizing

Pure Al and the Al-Si alloys were all melted in different laboratory scale electrical resistance furnaces. *The coating materials were; pure Al, pure Al-Si (7wt %), commercial Al-Si (7wt %) and pure Al-Si (12.5wt %).* Boron nitride coated fired clay crucibles were used for melting experiments. The temperature of the molten bath was monitored using a k-type thermocouple with a digital reader. The temperature of the furnaces was raised to 1023K until the entire pure Al and Al-Si alloys were completely melted. The temperature was then lowered and maintained first at 933K.

Before dipping the steel samples, the oxide layer that formed on top of the baths was removed manually. Each specimen was dipped into the molten pure Al and Al-Si alloy melts for 30 minutes. At the end of the dipping time, a new oxide layer was removed and the coated specimens were taken from the baths and allowed to cool in air to room temperature.

The bath temperature was then raised to 973K and monitored until the molten aluminium obtained the above temperature. Samples were dipped in the aluminium baths for 30 minutes after which the temperature was finally increased to 1023K. When the molten bath reached the desired dipping temperature, any oxide layer that was present on top of the melt was removed using a steel rod and the sample were immersed and kept in the bath for 30 minutes.

During dipping of the steel samples that had been kept in glycerol, a very rough coating was obtained in addition to its poor adhesion. To avoid the formation of an oxide layer on top of the bath, a second set of samples were dipped in a pure Al-Si (12.5wt %) bath which was fluxed with a molten mixture of 54wt% KCl and 46wt% NaCl. Due to the extremely corrosive nature of molten salts mixture, an alumina crucible was chosen to withstand both the molten aluminium and fluxing salt mixture. A thin layer of flux about 5cm was place on top of both the molten commercial and pure Al-Si (7wt %) alloys.

Fluxing with molten salts

The salt mixture was first dried and heated up to 873K in a fired clay crucible with a layer of aluminium foil placed on the inside. This prevented the introduction of moisture from the salts onto the bath which may cause a splash of molten metal and also it is a safety precaution not to add cold salt to a bath at high temperatures above 873K. In general, for safer operation, the temperature difference between the salt and the molten bath should be as small as possible. At this temperature the aluminium foil did not melt. Using the salt fluxed prevented any kind of oxide layer on top of the baths but in this experiment no preheating was done of the samples and therefore cold sample were immersed. As a result, a layer of salt froze around the sample and at the end of the dipping time; some areas were not wetted by the molten aluminium alloy resulting in some parts being well aluminized and others were left bare. When the coated samples were taken from the salt fluxed baths, they had a layer of salt that cooled very fast, was very hard and tough to remove.

The experimental set up was not constructed to simulate the industrial aluminizing process whereby there is a molten salt bath which is kept at the same temperature as the coating temperature. This serves for both chemical cleaning of the steel samples and preheating them in

an air-free environment and from here the hot, clean samples continue to the coating tank which is also fluxed at the top. The samples move throw the aluminizing bath which also helps to rinse off any salts that may have stuck onto the surfaces of the substrates.

Sample withdrawal

It has been mentioned in the literature [24] that the speed of withdrawal of the samples from the bath influenced the physical quality of the coating layer.

It was also observed that when the samples were taken out relatively fast and with a steady hand, a smooth outer coating layer was obtained. A slow and shaky sample removal led to the newly formed oxide layer sticking on to the sample as it was withdrawn which made a very rough, uneven and discolored (tarnished) coating layer.

Immediately after removing the samples from the bath, excess aluminium was wiped from the lower end of the samples while it was still liquid.

Surface preparation

The aluminized samples were sectioned using a Struers Discotom-5 cutting machine, mounted using ClaroCit powder mixed with ClaroCit liquid resin followed by grinding with silicon carbide paper numbers from 320-4000. Polishing was done using an automatic polishing machine (Struers tegrapol-31) using DP-Mol and DP-Nap fabric with suspensions of 3 and 1 μm for 1 minute at each step to obtain a scratch-free and clean surface. The polished specimens were etched in 2% Nital solution for about 5 seconds, rinsed with water followed by ethanol and dried rapidly.

Optical microscopy

Microscopic examination of these specimens was carried out using an optical light microscope (LEICA MEF4M) fitted with a digital camera. Under the optical light microscope the thickness and morphology of the coating and intermetallic layers were studied.

SEM imaging

The polished and etched specimens were then characterized using the scanning electron microscope (LVFESEM Zeiss Supra 55VP). The scanning electron microscope (SEM) uses a

focused beam of high-energy electrons to generate a variety of signals at the surface of solid specimens. The signals that derive from electron-sample interactions reveal information about the sample including external morphology (texture), chemical composition, and crystalline structure and orientation of materials making up the sample.

Accelerated electrons in an SEM carry significant amounts of kinetic energy, and this energy is dissipated as a variety of signals produced by electron-sample interactions when the incident electrons are decelerated in the solid sample. These signals include secondary electrons that produce SEM images, backscattered electrons (BSE), diffracted backscattered electrons (EBSD) that are used to determine crystal structures and orientations of minerals, photons (characteristic X-rays that are used for elemental analysis and continuum X-rays), visible light (cathodoluminescence--CL), and heat.

EPMA

The polished surface of the samples was coated with a thin layer of carbon dust and the rest of it was wrapped in aluminium foil to ensure a good conductance before loading them onto the sample holder of the JXA-8500F Field Emission Electron Probe micro analyzer. Imaging, mapping and point analysis was done by selecting several random points in each distinct alloy phase. The EPMA's principle of operation involves bombarding a micro-volume of a sample with a focused electron beam (typical energy = 5-30 keV) and collecting the X-ray photons thereby emitted by the various elemental species. Since the wavelengths of these X-rays are characteristic of the emitting species, the sample composition can be easily identified by recording WDS spectra (Wavelength dispersive spectroscopy).

XRD Analysis

Three samples were cut from the aluminized steel for analysis using a Siemens D5000 X-ray Diffractometer. No metallographic sample preparation was done to the first sample, the second and third samples were carefully prepared with fine grinding steps using 2400 followed by 4000 SiC paper to expose the underlying coating and intermetallic layers respectively. X-ray scattering technique is one of the non-destructive analytical techniques which reveal information about the crystal structure, chemical composition, and physical properties of materials and thin films.

These techniques are based on measuring the scattered intensity of an X-ray beam hitting a sample as a function of the incident and scattered angle, polarization, and wavelength or energy.

Micro hardness

A Vickers hardness test was conducted using the LEICA/MHT MOT micro hardness tester at a magnification of x50, a 50gf load for 15s. The micro hardness tester is equipped with a diamond indenter in form of a square-shaped pyramid capable of producing geometrically similar impressions, irrespective of size.

The basic principle, as with any hardness measurements is to study a material's ability to resist plastic deformation from a standard source. There are different kinds of hardness tests but the Vickers test was used for all coated steel samples because it has one of the widest scales. An indentation is made on the test sample's surface for a given load and magnification, then the length of diagonals (d_1 and d_2) of the indentation are measured. The Vickers hardness is calculated using the equation below,

$$HV = 1.854\ P/d_1^2$$

Where P is the load in Kg, d_1 is the length of diagonal of impression in mm.

4. Experimental results

After the hot-dipped steel strips cooled, it was observed that a continuous, uniform coating layer covered the strips. Some of the steel strips hot-dipped in pure aluminium developed a light brown colour on cooling while the samples coated with Al-Si alloys maintained a grey shinny coating. The coating however became slightly rough once the samples were shaken before the aluminium alloy on the surface had completely solidified. The coated samples therefore must be transferred carefully out of the coating bath to a place where they cool to room temperature.

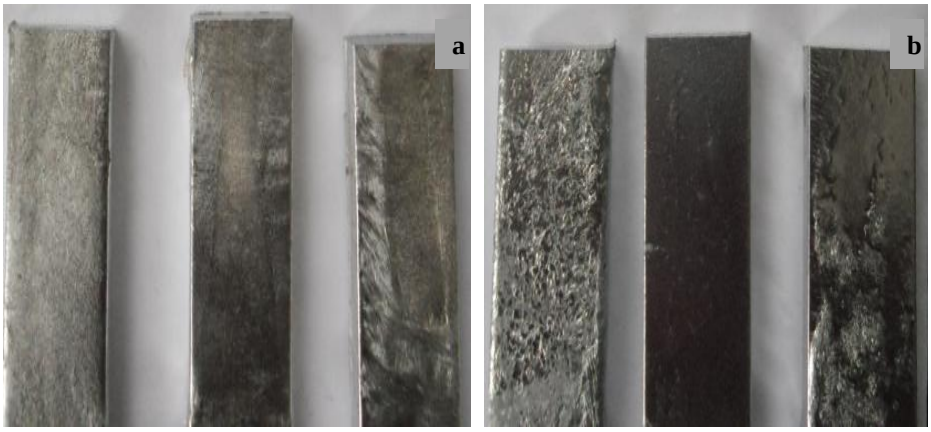

Figure 9: Coating results of steel strips hot-dipped in (a) molten pure aluminium and (b) Al-Si 12.5wt% alloy

Optical light microscopy

The images of cross sections obtained from the optical light microscope for samples aluminized by hot dipping in pure aluminium and in the three Al-Si alloys, showed an increase in the thickness of intermetallic layer for higher dipping temperatures.

A single phase with finger-like morphology of intermetallic phase was present for samples coated in pure aluminium, while a planar front with two different phases was formed in samples coated with Al-Si alloys. Figure 11 below shows images from optical light microscopy showing the coating, intermetallic and steel substrate phases respectively from the left to the right in each image.

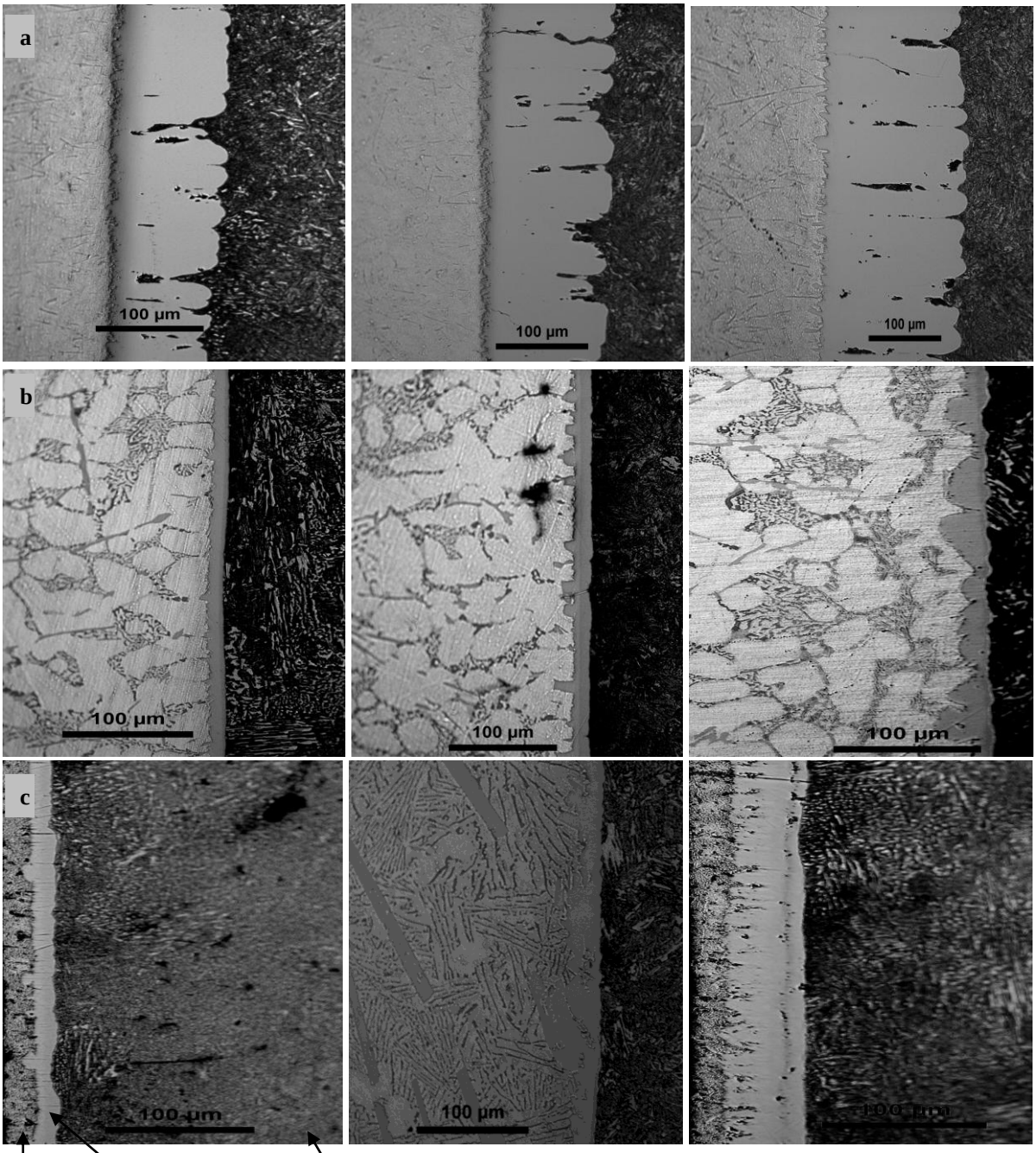
a
100 µm
100 µm
100 µm
b
100 µm
100 µm
100 µm
c
100 µm
100 µm
100 µm
Coating
intermetallic
steel

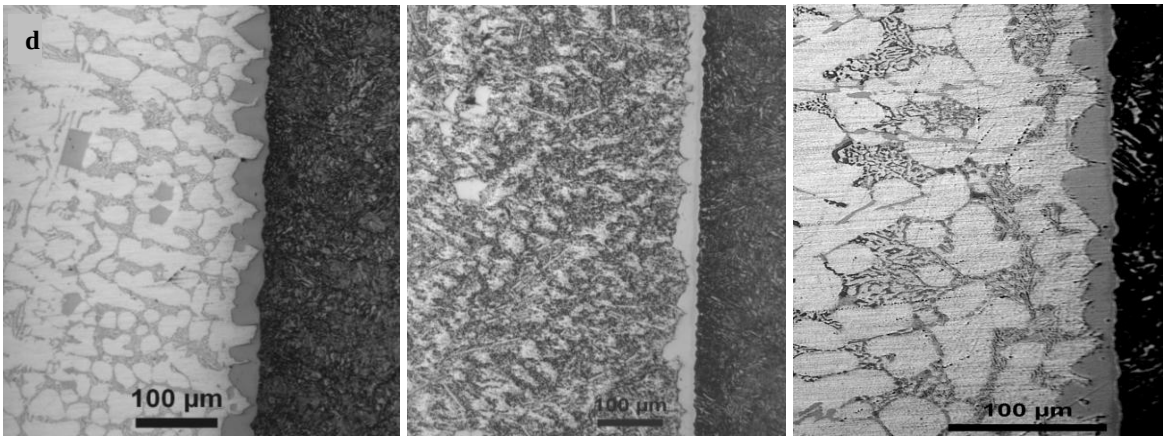

Figure 10: Optical light micrographs showing coating and intermetallic layers of samples hot dipped in pure aluminium and Al-Si alloys for 30 min at 933, 973 and 1023K

Image ***a*** , ***b, c*** and ***d*** show cross sections of samples hot-dipped in pure al, pure Al-Si (12.5wt%), commercial Al-Si(7wt%) and pure Al-Si(7wt%) respectively.

SEM imaging

Image of cross sections obtained from the scanning electron microscope show one Fe_xAl_y alloy phase formed in the intermetallic layer between pure Al and iron in the steel phase (image *a*) while two or three $Fe_xAl_ySi_z$ alloy phases are formed between Al-Si in the melts and iron(images *b-d*).

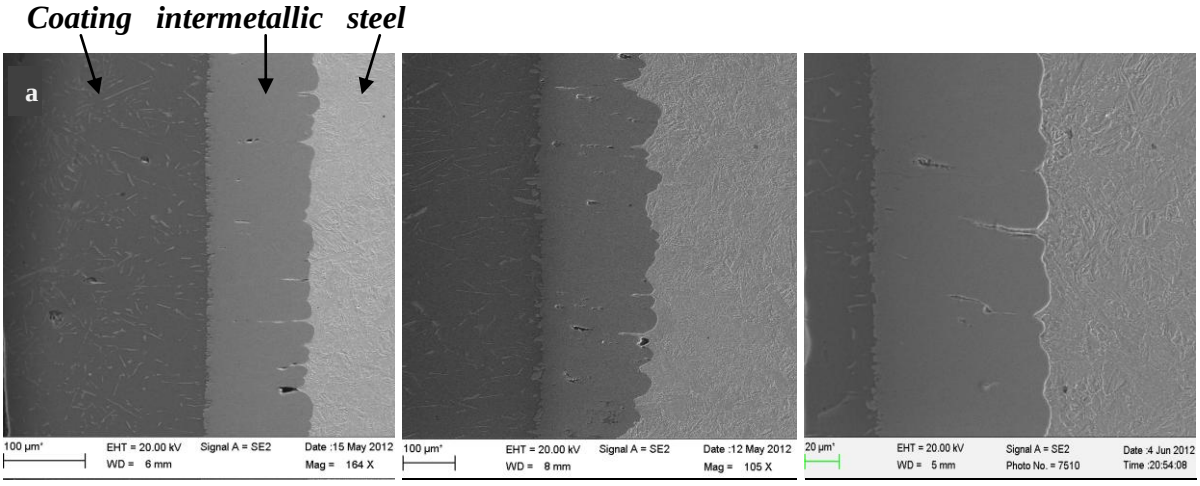

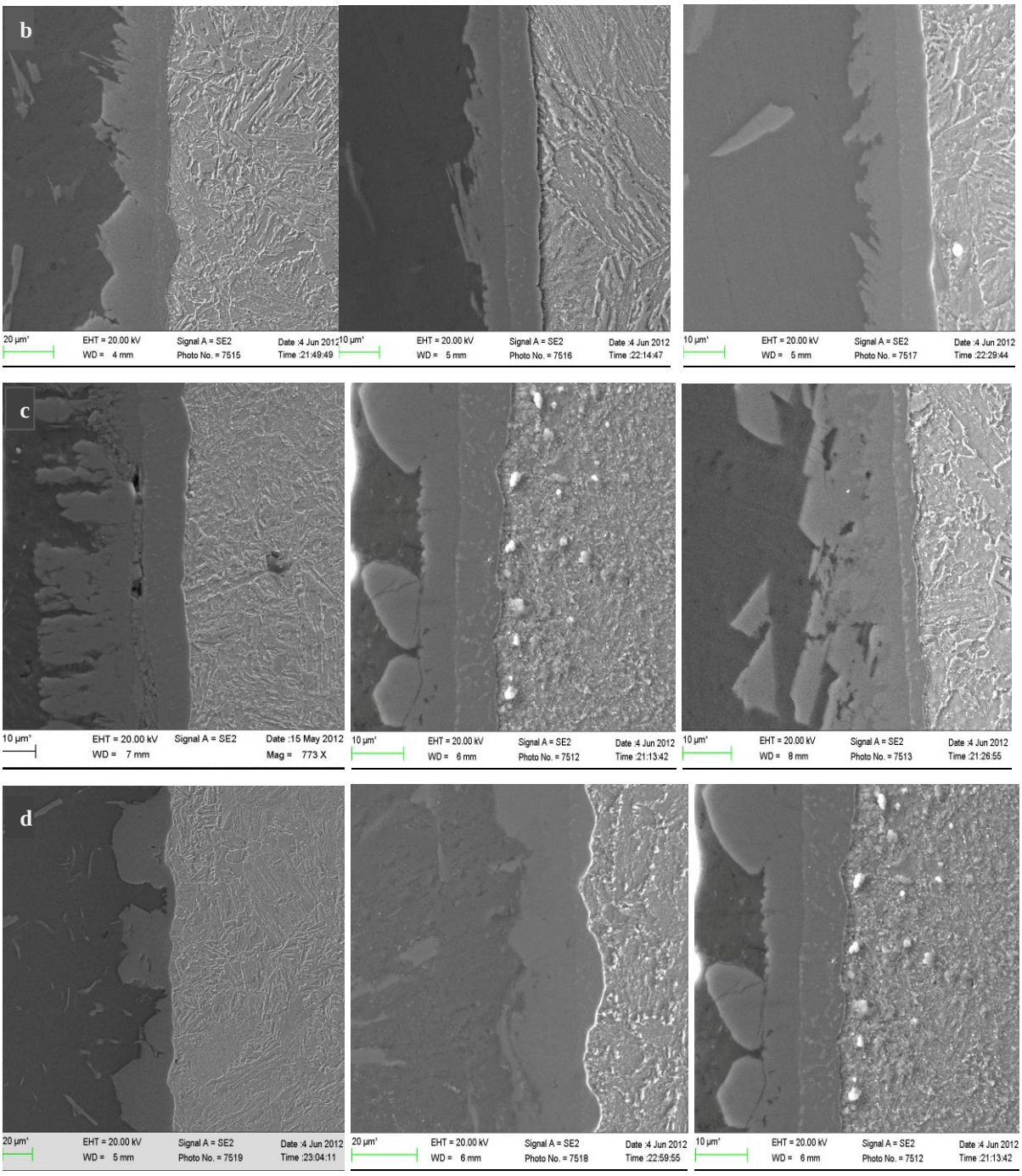

Figure 11: SEM micrograph showing phases of coating layer for sample dipped in pure Al and Al-Si alloys for 30 min at 933, 973 and 1023K.

Image ***a***, ***b, c*** and ***d*** show cross sections of samples hot-dipped in pure Al, pure Al-Si (12.5wt %), commercial Al-Si (7wt %) and pure Al-Si (7wt %) respectively. The images are of samples hot dipped at 933, 973 and 1023K from left to right.

Coating and intermetallic layer thickness

Values obtained of the coating and intermetallic layer thickness show that both layers increase in thickness at higher dipping temperatures. The intermetallic layer for samples hot-dipped in pure aluminium is about 38% of the total coating. The interlayer thickness formed between Al-Si and steel is 5-7% of the total coating. Samples dipped in pure Al-Si 12.5wt% melt have the lowest coating layer thickness.

Table 6: Average thickness of intermetallic layer for steel samples dipped in Al and in Al-Si alloy baths.

(a) Dipping in a pure aluminium bath

Dipping temperature (K)	Alloy phase thickness (µm)	Coating layer thickness (µm)
933	105.0	166.4
973	143.4	229.7
1023	189.1	239.8

(b) Dipping in pure Al-Si 12.5wt% alloy

Dipping temperature(K)	Alloy phase thickness (µm)	Coating layer thickness (µm)
933	15.2	45.8
973	22.1	35..2
1023	34.6	51.1

(c) Dipping in pure Al-Si 7wt% alloy

Dipping temperature(K)	Alloy phase thickness (µm)	Coating layer thickness (µm)
933	-	-
973	34.5	423.1
1023	37.5	598.5

(d)Dipping in commercial Al-Si 7wt% alloy without salt flux

Dipping temperature(K)	Alloy phase thickness (µm)	Coating layer thickness (µm)
933	12.8	256.1
973	19.6	297.1
1023	32.0	443.8

(e) Dipping in Commercial Al-Si 7wt% alloy with salt flux

Dipping temperature(K)	Alloy phase thickness (µm)	Coating layer thickness (µm)
933	-	307.5
973	26.5	460.2
1023	33.6	647.0

Micro hardness

Figure 12 below shows some of the impressions created in the intermetallic layer of the aluminized steel test samples. Images *a*, *b* and *c* are of cross sections of steel samples hot-dipped in pure Al-Si (12wt %) at 1023K, pure Al at 973K and pure Al at 1023K.

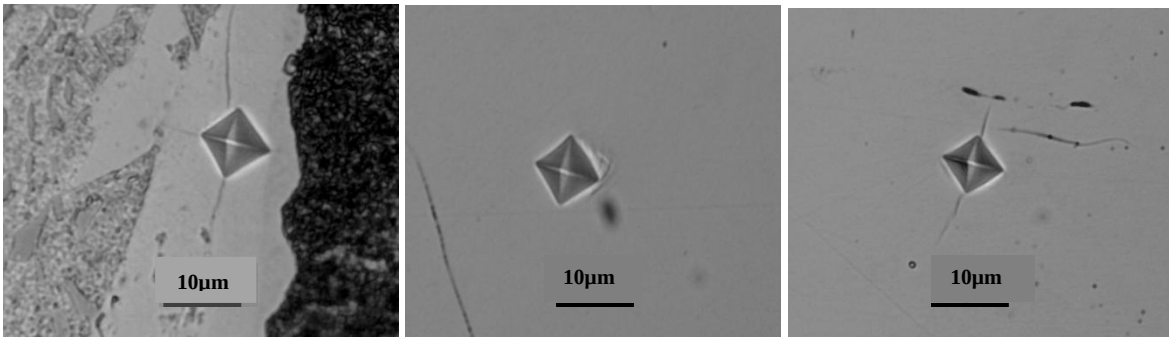

Figure 12: Indentations made during micro hardness testing of the alloy phases formed during hot-dip aluminizing.

Table 7: Micro hardness (HV) for the different intermetallic phases

Temperature (K)	pure Al	pure Al-Si (12.5wt %)	commercial Al-Si (7wt %)	pure Al-Si (7wt %)
1023	958	715	645	685
973	918	688	-	755
923	941	702	-	-

The intermetallic layer formed between pure aluminium and steel had average vickers hardness values above HV 900 compared to the average hardness of the aluminium coating layer of about HV50 and that of the steel about HV290 obtained in this study. Some samples had very thin intermetallic phases that during indentation, the square-based pyramid impression was made across different alloy phases and hence the hardness could not be determined for a single phase.

EPMA imaging, mapping and point analysis

Figure 13 below shows back scattered images of cross sections for hot-dip aluminized steel samples.

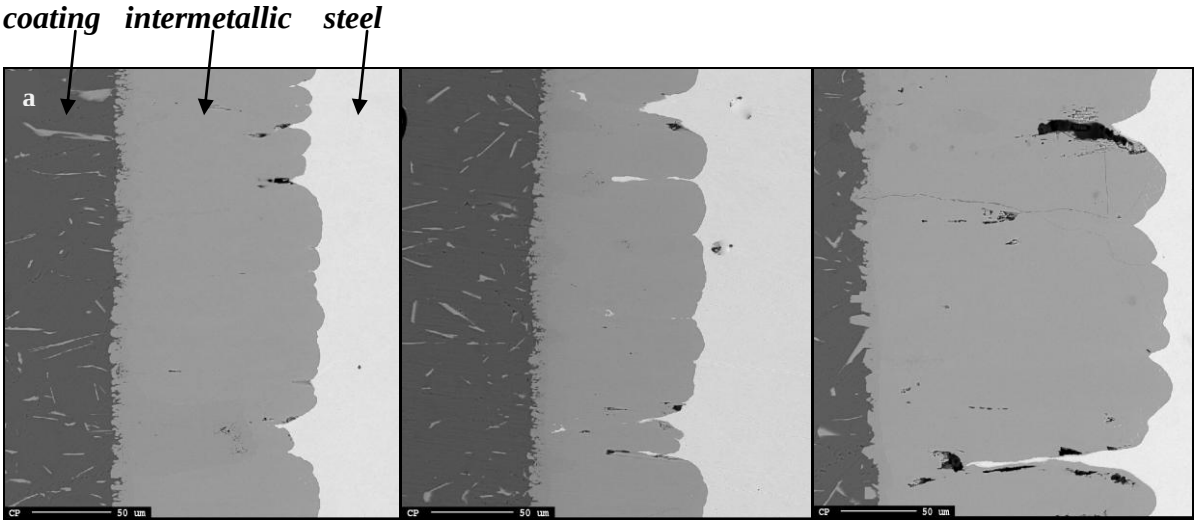

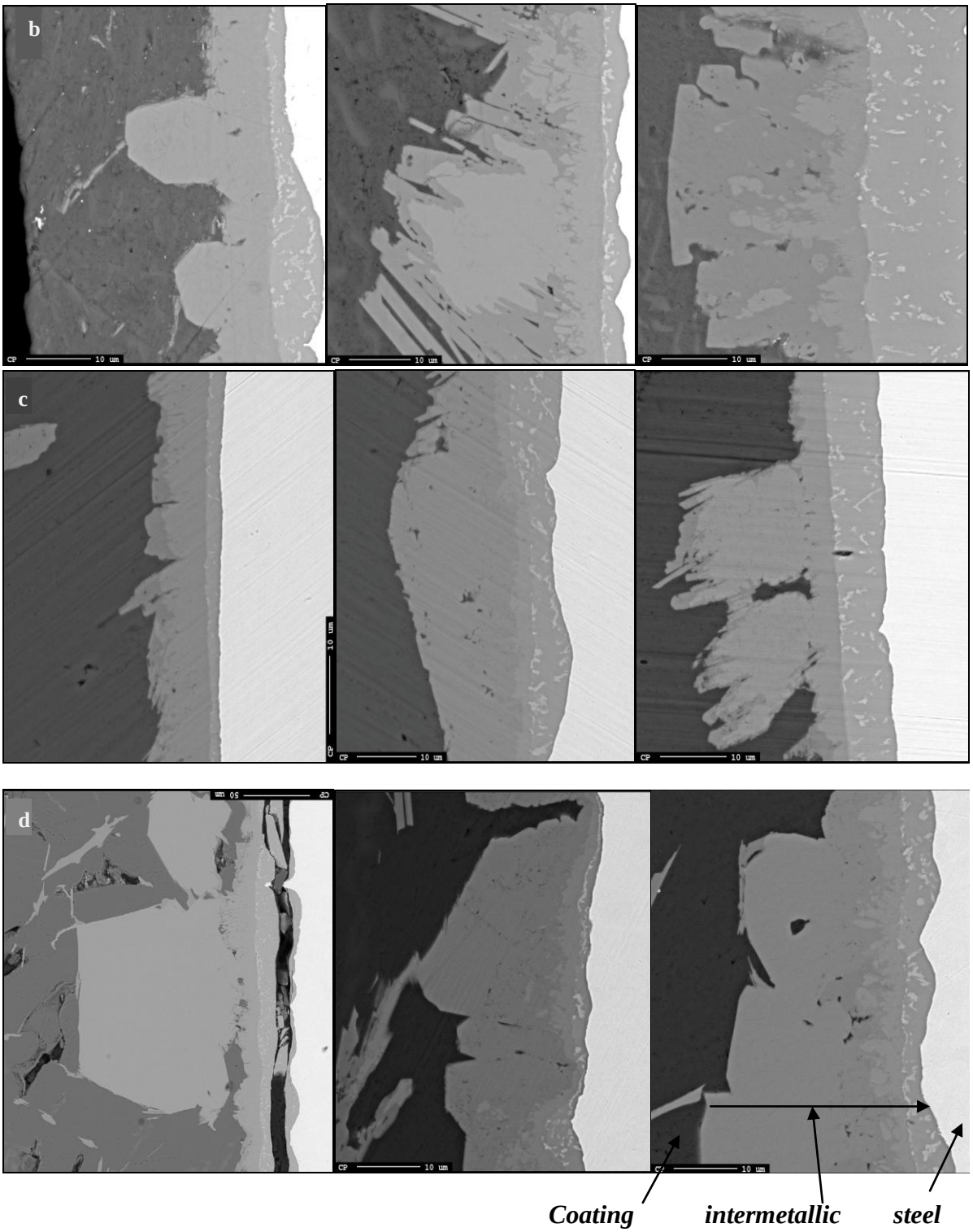

Figure 13: EPMA images of the cross section of coating and intermetallic layer of steel strips of samples dipped in pure Al and Al-Si alloys for 30 min at 933, 973 and 1023K.

Image ***a***, ***b, c*** and ***d*** show cross sections of samples hot-dipped in pure Al, pure Al-Si (12.5wt %), commercial Al-Si (7wt %) and pure Al-Si (7wt %) respectively. The images are of samples hot dipped at 933, 973 and 1023K from left to right.

In the images above, cross sections of the steel samples hot dipped in the three different Al-Si alloy melts, have at least three phases of different compositions within the intermetallic layer. The relative compositions in mass% were determined through point analysis and the distribution of elements was obtained through mapping.

Mapping

Distribution of elements across the cross sections of the hot-dip aluminized samples is shown in the images below.

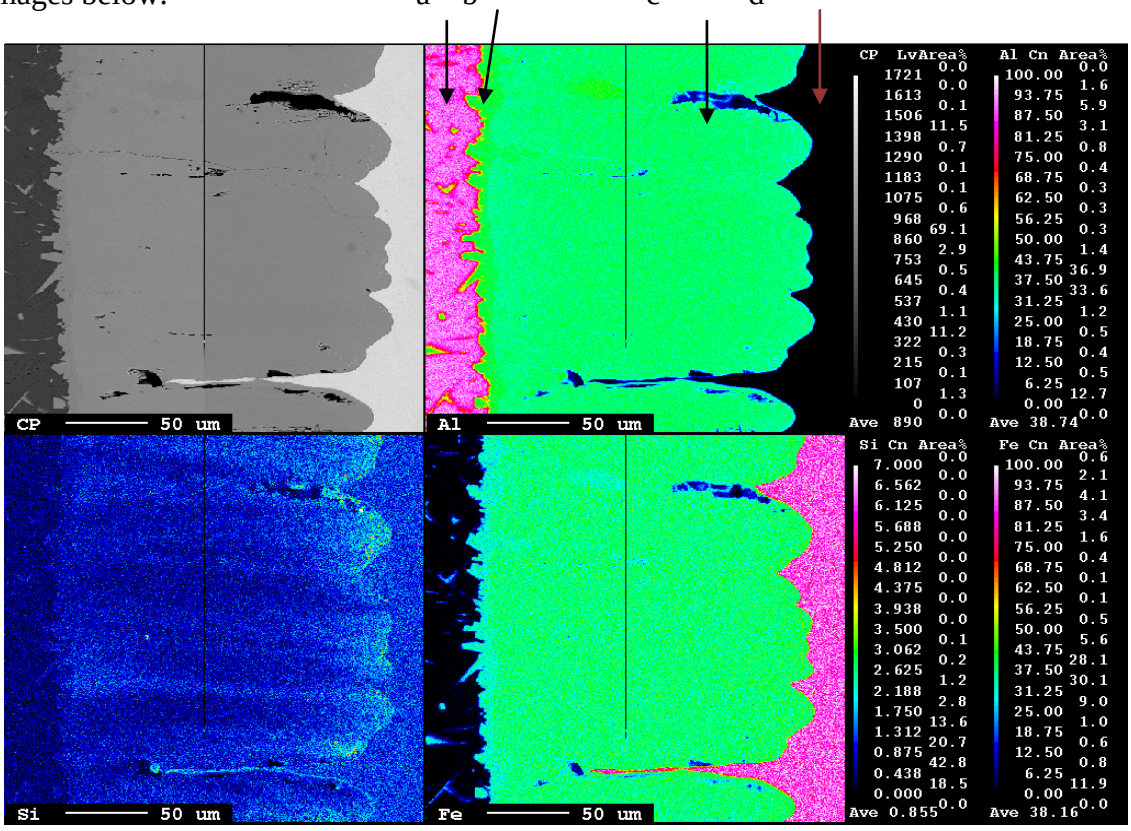

Figure 14: EPMA mapping showing distribution of elements in steel strip hot-dipped in pure Al at 1023K for 30 min

Table 8 :Point composition for sample hot-dipped in pure Al at 1023K for 30 min

Region	Al mass	Fe mass	Total mass	Fe (mass %)	Al (mass %)
a	101.538	0.199	101.737	0.196	99.804
a	100.087	0.407	100.494	0.405	99.595
a	100.193	0.799	100.992	0.791	99.209
b	59.819	37.353	97.172	38.440	61.560
b	59.267	37.518	96.785	38.764	61.236
b	59.037	38.865	97.902	39.698	60.302
c	55.243	41.834	97.077	43.094	56.906
c	57.294	42.39	99.684	42.524	57.476
c	57.796	41.897	99.693	42.026	57.974
c	55.773	42.954	98.727	43.508	56.492
d	0.529	95.673	96.202	99.450	0.550
d	0.035	94.625	94.66	99.963	0.037

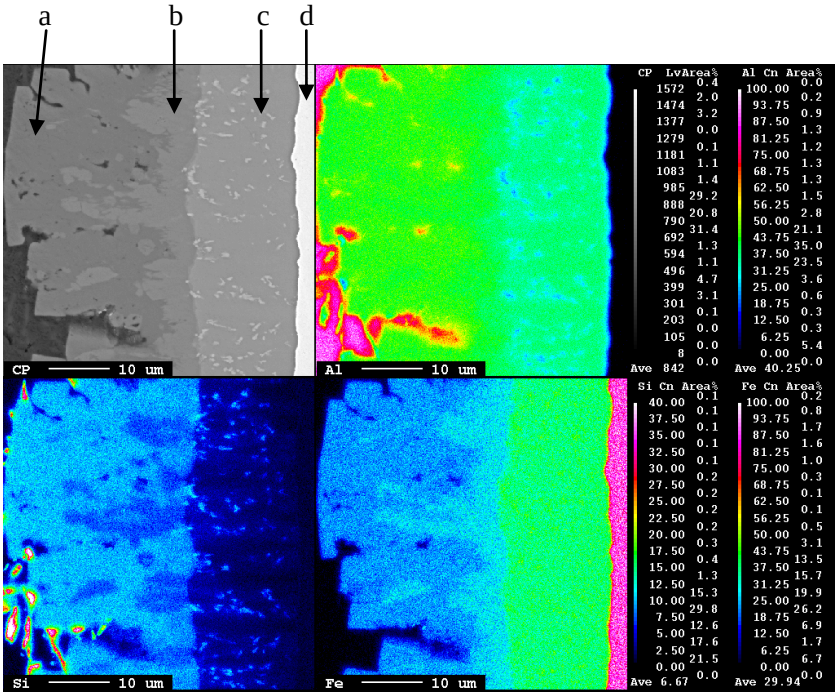

Figure 15: EPMA mapping showing distribution of elements in steel strip hot-dipped in pure Al-Si 12.5wt% alloy at 933K for 30 min

Table 9: Point Composition of samples hot dipped in pure Al-Si 12.5wt% alloy at 933K for 30 min

Region	Al	Fe	Si	total	Al (mass%)	Fe (mass%)	Si (mass%)
a	97.179	0.699	1.338	99.216	97.947	0.705	1.349
a	96.782	0.977	1.876	99.635	97.137	0.981	1.883
b	57.552	26.276	16.291	100.119	57.484	26.245	16.272
b	58.336	25.173	15.58	99.089	58.872	25.404	15.723
b	57.294	31.719	10.789	99.802	57.408	31.782	10.810
c	52.576	41.253	4.793	98.622	53.311	41.829	4.860
c	54.929	43.392	2.009	100.33	54.748	43.249	2.002
d	0.243	95.023	0.684	95.95	0.253	99.034	0.713

X-ray diffraction

Spectra of the outer coating layer and intermetallic layer of samples hot dipped in pure Al show that a passive aluminium oxide layer is formed on top of the coating layer and the two alloy compounds are formed between Al and Fe , Fe_2Al_5 and $FeAl_3$ and the main coating layer is only Al. Several phases are formed between iron and Al-Si and other elements present in the melt such as Mn and Mg. Some of the alloy compounds are *FeSi, AlFeSi, Al_5FeSi and $Al_{0.7}Fe_3Si_{0.3}$*

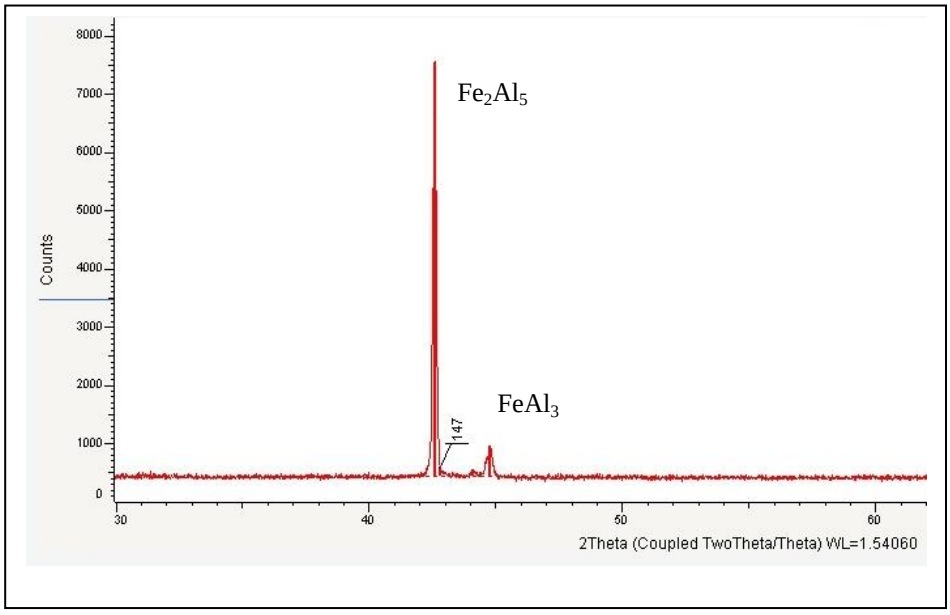

Figure 16: XRD spectrum of Intermetallic layer for sample hot dipped in pure Al at 1023K

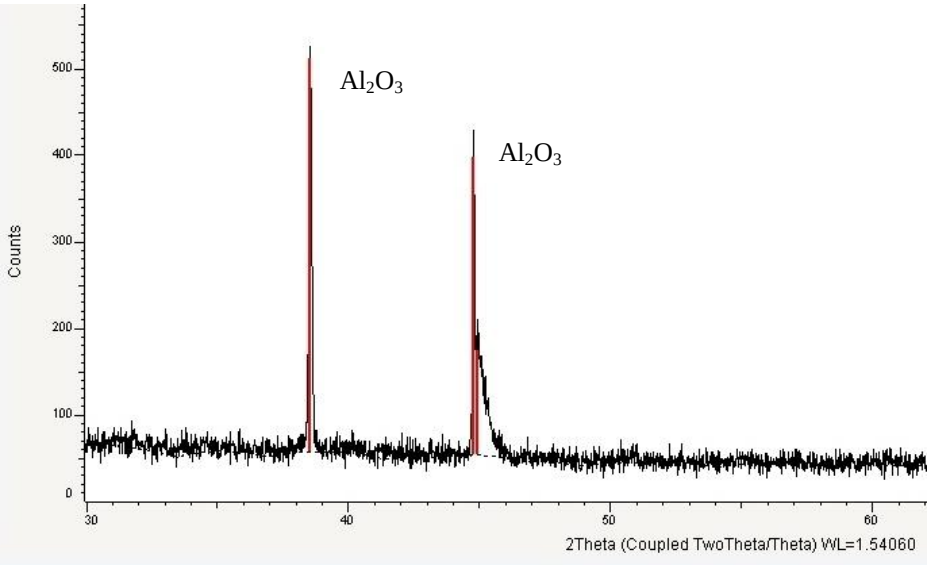

Figure 17: XRD spectrum of external coating layer for sample hot dipped in pure aluminium at 1023K

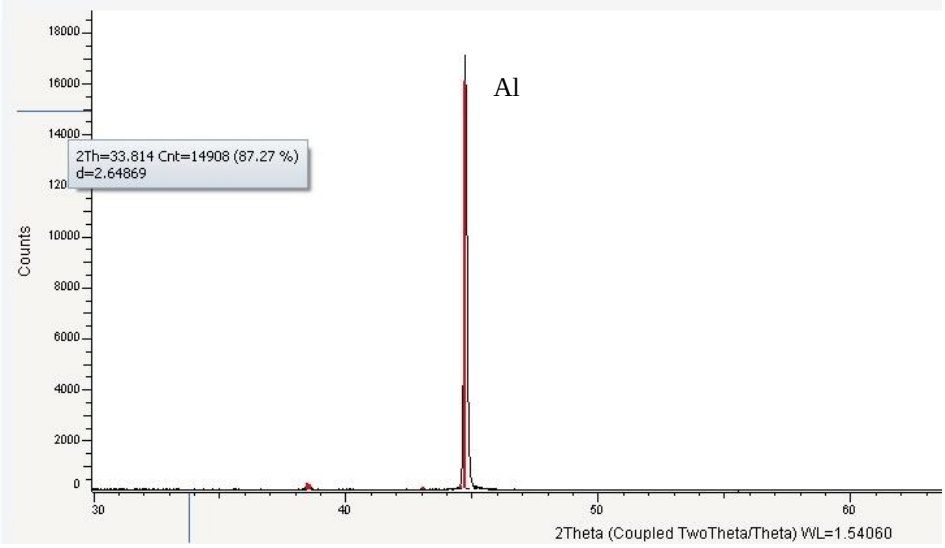

Figure 18: XRD spectrum of coating layer for sample hot dipped in pure Al at 1023K

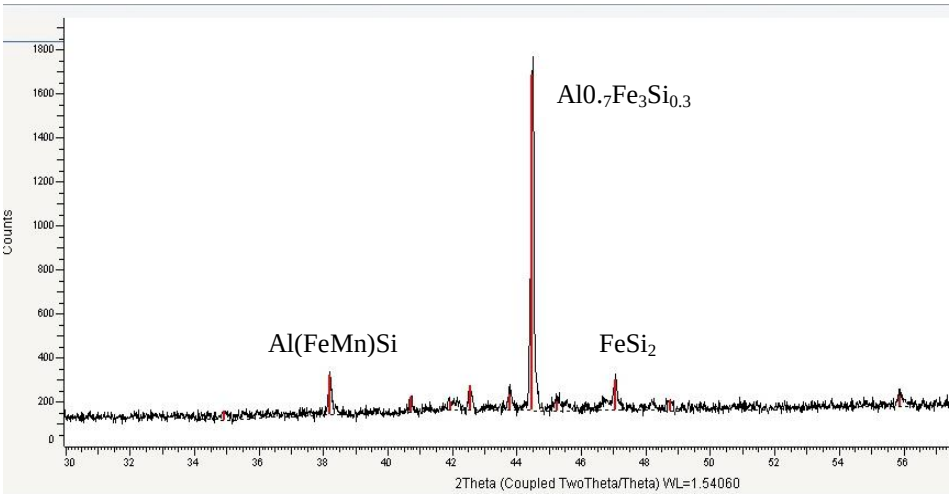

Figure 19: XRD spectrum of outer coating layer for sample hot dipped in pure Al-Si (12.5wt %) at 1023K

5. Discussion

Purpose of hot-dip aluminizing

The primary objective for aluminizing steel is to improve the surface properties of the steel such as heat resistance and reflectability, corrosion and oxidation resistance mostly for applications at elevated temperatures from 723-1123K but other benefits are achieved due to the formation of the intermetallic layer between the coating aluminium layer and the steel substrate which improves the surface hardness of the plain low carbon steel from about HV 250 to above HV 600.

This makes the steel more abrasion and wear resistant. However the harder intermetallic layer is more brittle and not suitable for fabrications that involve forming and other kinds of plastic deformation due to reduced ductility. During such processes the intermetallic layer that consists of different Al_x-Fe_y or Al_x-Fe_y-Si_z, may undergo brittle fracture, developing cracks that could propagate through the steel phase and leading to failure. Aluminizing is done at temperatures above 873K which also reduces the strength properties especially under tensile stress.
Plain Carbon steel hot dipped in Si-Al alloy is best suited in an environment where a combination of heat and corrosion is involved.

Steel hot-dipped in pure Al has excellent resistance to atmospheric corrosion. Aluminized steel coated with Al-Si has better heat and oxidation resistance up to 775K without discoloring and maintains its strength at temperatures up to 940K and is also a cost effective alternative to stainless steel since it frequently maintains its appearance better in service than for example 409 stainless.
Aluminized steel shows excellent heat reflectivity during exposures below 755K, reflecting up to 80% of the radiant heat that strikes it.
It is therefore advisable to aluminize steel parts with Al-Si alloys where the strength properties are not critical for its final application like in heating elements, industrial waste exist streams and automobile mufflers.

Coating

In the coating experiments, steel samples were dipped in pure Al and three different Al-Si alloys for 30 minutes at temperatures 933, 973 and 1023K. It should however be noted that different surface preparation was done for some of the steel samples prior to hot-dipping.

For all the dipping temperatures, an intermetallic phase was formed as a result of a chemical reaction between the iron in the steel phase and the aluminium in the coating layer. The above reaction only took place when the steel was wetted by the aluminium melts.

The intermetallic layer thicknesses for all samples coated with pure Al and with the different Al-Si alloys increased with higher dipping temperature as seen in table 5 and in the figures 8 and 9 which was in agreement with the results reported in other studies [9].It was observed in this study that there was discontinuity in development of the intermetallic layer for the samples that were immersed in a commercial Al-Si alloy melt fluxed with molten salts at 933K. When cold steel strips were immersed in the coating melt at 933K, the molten salt froze over the steel surface and did not melt away in some areas which made it impossible for the molten aluminium to wet the steel. In the laboratory setup, the strips were not in constant motion through the coating bath like in industrial processes but are in a single position throughout the hot dipping experiment.

There was no wetting of the steel, which led to limited reaction between the aluminium melt and the steel in those regions and therefore the intermetallic phase was absent.

The samples immersed in a fluxed bath had a higher thickness of the coating layer thickness than the samples dipped in the unfluxed bath as seen in the summarized table 6 (d) and (e).

Formation and composition of coating layer and intermetallic phases

The images obtained from the optical light microscope and SEM indicated that there was one alloy phase formed between the coating layer and the steel for specimens dipped in the pure Al.

However, images obtained by EPMA show a second phase present between the aluminium coating layer and the main alloy phase which is next to the steel. This intermetallic phase is very thin and has a higher Al content as seen in figure 14.

EPMA images obtained from samples hot-dipped in Al-Si alloys had a coating layer and three distinct intermetallic phases for samples hot-dipped in the three aluminium-silicon alloys.

The coating layer consisted only of aluminium (99.5mass %) and a trace amount of Fe, less than 0.5 mass% was present for samples hot-dipped in pure aluminium. In cross sections of samples hot-dipped in the Al-Si alloys, the coating layer consisted of Al, Si and Fe.

Spectra obtained from x-ray diffraction show that two phases rich in aluminium (Fe_2Al_5 and $FeAl_3$) are formed between pure aluminium and iron in the steel, with Fe_2Al_5 being the main phase. A passive aluminium oxide (Al_2O_3) layer was formed on top of the coating aluminium layer. Several different phases were detected as present for samples hot-dipped in Al-Si alloys however each alloy layer is very thin and the first phases are not planar so obtaining one pure alloy phase during grinding for analysis by x-ray diffraction is a challenge. This is also the case during determination of micro hardness.

Iron in the aluminizing melt

The content of Fe in the coating layer may increase as more steel strips are hot- dipped in the pure aluminium or Al-Si alloy bath due to the rise in the amount of iron in the bath especially at higher temperatures above 973K. In the aluminium coating bath, iron content in excess of 2% is reported to produce rough coatings [24].The iron content introduced in the coating bath may however be controlled by operating at a lower bath temperature or by removing part of the bath and adding iron-free aluminum or aluminium alloy.

After coating 3 steel strips in a pure aluminium bath, the remaining molten aluminium was casted and left to cool. It was later sectioned, grinded and polished. A conductivity test carried out at six different points on the polished cast sample. The obtained results are given in table 10 below.

Table 10: Conductivity of aluminium cast after hot-dipping of steel

point	1	2	3	4	5	6
κ (µS/m)	51.3	51.9	51.8	51.7	51.9	52.2

The conductivity of pure aluminium according to the International Annealed Copper Standard at 100% is equivalent to 58.0 x 10^{-6} S/m. It is evident that there was a significant reduction in conductivity of the aluminium which was primarily attributed to the introduction of Fe from the steel into the coating melt. Fresh pure aluminium was melted for other hot-dip experiments.

Morphology of intermetallic layer

The main intermetallic phase formed in the steel strips dipped in pure aluminium had a ragged front which progressed with a finger like growth morphology into the steel substrate. This phase becomes less ragged and thicker with increase in temperature but develops more cracks at dipping temperature of 1023K. There are three intermetallic phases for samples dipped in the Al-Si alloys. The alloy phase immediately after the steel (d-phase) has a planar and smooth front, just after this phase, is the c-phase that is smooth on one side and ragged on the side closer to the b-phase, which is closer to the coating layer which is more ragged and has a very irregular thickness. This is followed by the Al-Fe-Si coating layer.

The presence of silicon in the aluminizing bath was reported to inhibit the rapid solid-state growth of the brittle Al-rich alloy phases such as the $FeAl_3$ and Fe_2Al_5 [18]. The total thickness of intermetallic layers formed between Fe and Al-Si alloys was much lower than that formed between the pure Al and Fe. It is in agreement with the earlier studies that have reported that the presence of silicon resulted in a reduced alloy phase thickness. The reduced alloy layer thickness is desirable in order to have a longer useful life of the coating. The intermetallic layer is harder and more brittle than the coating layer which makes it susceptible to brittle fracture and renders aluminized steel unsuitable for further processing that involves various forms of plastic deformation.

$Al_xFe_ySi_z$ phases formed between iron and Al-Si alloys have lower hardness and perform better than the harder more brittle $FeAl_3$ and Fe_2Al_5 phase formed with pure aluminium. This make Al-Si alloys a better choice of aluminizing material. To obtain an intermetallic layer that is significantly thinner than the coating layer in pure Al melts like that formed in melts of aluminium alloys with silicon, the dipping time has to be much shorter. Some of the previous studies [9] have reported dipping times of only 5 minutes, although this is sufficient when samples

have been cleaned thoroughly and pre-heated in fluxing bath at temperature close to the dipping temperature.

Effect of dipping temperature

The coating and intermetallic layer thicknesses increase as the temperature is raised from 933 to 1023K for samples hot dipped in both pure Al and aluminium alloys with silicon. For samples coated with aluminium-silicon alloys, some of the phases become thicker than others at higher temperature. For example the sample coated in commercial Al-Si (7wt%) at 1023K shows a thicker b-alloy phase immediately after the coating layer, which was common for all samples hot dipped in Al-Si alloys but the thickness of the d-alloy phase just after the steel, became thicker at a slower rate.

The chemical reaction between pure aluminium and iron leading to formation of Fe_xAl_y alloy compounds is rapid at temperatures below 973K, this implies that at higher temperatures it is more rapid and in addition the coating layer cools at a slower rate after withdrawal from the melt. During this time as long as the Al layer is still molten the reaction continues leading to a higher intermetallic thickness and a reduced the coating layer.

However in silicon enriched melts, a high dipping temperature leads to an increase in intermetallic layer but it is still much smaller compared to pure aluminium. This is bacause silicon inhibits the solid state growth of the intermetallic layer. It is therefore important to control the temperature of the melt during hot-dip aluminizing.

Size of crucible

During the hot dip aluminizing experiments different sizes of crucibles were used for coating. Using a crucible with a bigger inner diameter provided an area at the surface of the melt towards the center that was free of the oxide layer. The formation of the oxide layer is more rapid at the walls of the crucible and progresses towards the centre. After removing the oxide layer, a quick immersion of the steel sample was possible without interference from the passive oxide layer.

Hardness

The $Al_xFe_ySi_z$ alloy compounds had lower vickers hardness values between HV 750 and 650 as compared with Al_xFe_y phases in samples coated with pure Al with values above HV900 and are more brittle.

6. Conclusion

The following conclusions have been drawn from the course of this work:

1. During hot-dip aluminizing of plain carbon steels an intermetallic layer is formed due to a chemical reaction between molten pure aluminium or an aluminium alloy and the iron in the steel.

2. The intermetallic layer formed during hot-dip aluminizing in molten pure aluminium may consist of either a single phase or more than one phase depending on the dipping temperature and time. The coating and intermetallic layer thickness increases with increasing dipping temperature and dipping time.

3. Dipping temperature of 973K is sufficient for hot-dip aluminizing processes.

4. A dipping time of 30 minutes was very long for hot-dipping in pure Al and allowed for the formation of a very thick intermetallic layer even at the lower dipping temperature of 933K. The alloy layer which was mainly Fe_2Al_5 obtained surface defects mostly cracking during the metallographic surface preparation. In addition, long dipping times lower some critical properties of the steel like fatigue strength.

5. For steel samples that have been mechanically and chemically cleaned and preheated in an oxygen free environment for about 5 minutes, a maximum dipping time of 10 minutes could be sufficient to produce a uniform and continuous aluminium coating layer.

6. Dipping time may however be longer for Al-Si alloy melts since the growth of intermetallic layer is slower.

7. Presence of silicon in the aluminium melt produces a significantly thinner and planar intermetallic phase that is less brittle compared to a thicker and ragged intermetallic layer formed between steel coated with pure aluminium.

8. Chemical cleaning using an acid or a molten salt bath is beneficial and increases the wettability of the steel by the molten aluminium but every cleaning step increases the time and cost of the aluminizing process. Grinding or blasting with abrasive grit may be done instead.

9. Fluxing of the aluminium bath is used for sample preheating, surface cleaning and prevention of an oxide layer at the surface of bath.

10. Aluminizing as a surface treatment step may be recommended for applications such as heating elements, exhaust systems and in corrosive/ oxidizing environments but not for applications that may require the material to undergo plastic deformation or forming.

8. References

1. V.N Yeremoko, V.Y. Nantanzon and V. I. Dybkrov, Russ metal, 1973, Vol.5, p66
2. T.Heumann and S. Dittrich: Z.metallkunde,1959, Vol.50,p.617
3. R.W. Richards, R. D. Jones, P. D. Clements, and H. Clarke: Metallurgy of continuous hot dip aluminizing, International materials Review, 1994,Vol.39, No.5, p.191
4. U.R Kattner and T.B.Massalski: Binary alloy K.William: Encyclopedia Britannica, Bessemer process, 2005, Vol.6, p.791
5. A.K steel, www.aksteel.com/product/features site browsed on 20.09.2011
6. Atlas steel, www.atlasstel.com/products/aluminized steel.aspx site browsed on 15.10.2011
7. P.N. Bindumadhavan and S. Markesh: Surface and Coating technology, 2000, Vol. 127, pp. 251-258
8. V.R. Ryabov: Aluminizing of Steel, 1985 pp. 45-51
9. S.Kobayashi and T.yakou:Control of intermetallic compound layers, Materials Science and Engineering, 2002 Vol. A 338, pp 44-53
10. E.V. Aksenova and I.B. Serebryakova:Research institute of ferrous metals,1972 Vol.8,No.1
11. K. Schubert, Crystal structure of two component phases, springer-verlag berlin,1964
12. phase diagrams, ASM International material park,1990, p.147-149
13. M.Y. zaki: Aluminizing of plain carbon steel, University of Engineering and Technology, Lahore, unpublished research, 2011.
14. M. Johnson, D. Mikkola and P.A. March: 1990, Vol 140, pp.279-289
15. M.Sundqvist and S.Hogmark: Tribol.Int,1993 Vol.26, pp129-134
16. J.E.Nicholls: corrosion technology,1964, Vol.11, pp.16-21
17. N.Komatsu, M.Nakamura and H.Fugita: J.Jpn.inst.met,1955, Vol.19, pp 416
18. G.Eggeler, W.Auger and H.Kaesche: Influence of silicon on growth of alloy layer during hot-dip aluminizing, 1986, Vol.21, no.9

19. T.Shih shih and T. Shu-Hau: Journal of Materials Science and Engineering, 2007, A Vol.454-455, pp.329-356
20. T.Morinaga and Y. Kato: Jpn. Inst. Met, 1955, Vol.19, p.578
21. M.V. Akdeniz and A.O Mekhrabov: Acta mater, 1998,Vol.46,p.1185
22. www.steel-grades.com/Steel-grades/Carbon-steel/g10400 site browsed on 20.02.2012
23. James F. Jenkins P.E www.events.nace.org/library/corrosion/metal coatings/ cladding.asp
24. Gul H. Awan, The morphology of coating-substrate interface in hot-dip aluminized steel, 2001.
25. ASM Handbook committee; Aluminum coating of Steel, ASM metals Hand Book, on Surface Cleaning, Finishing and Coating, ASM International, Material Park, OH, 5(1982) 335-347

9. Appendix

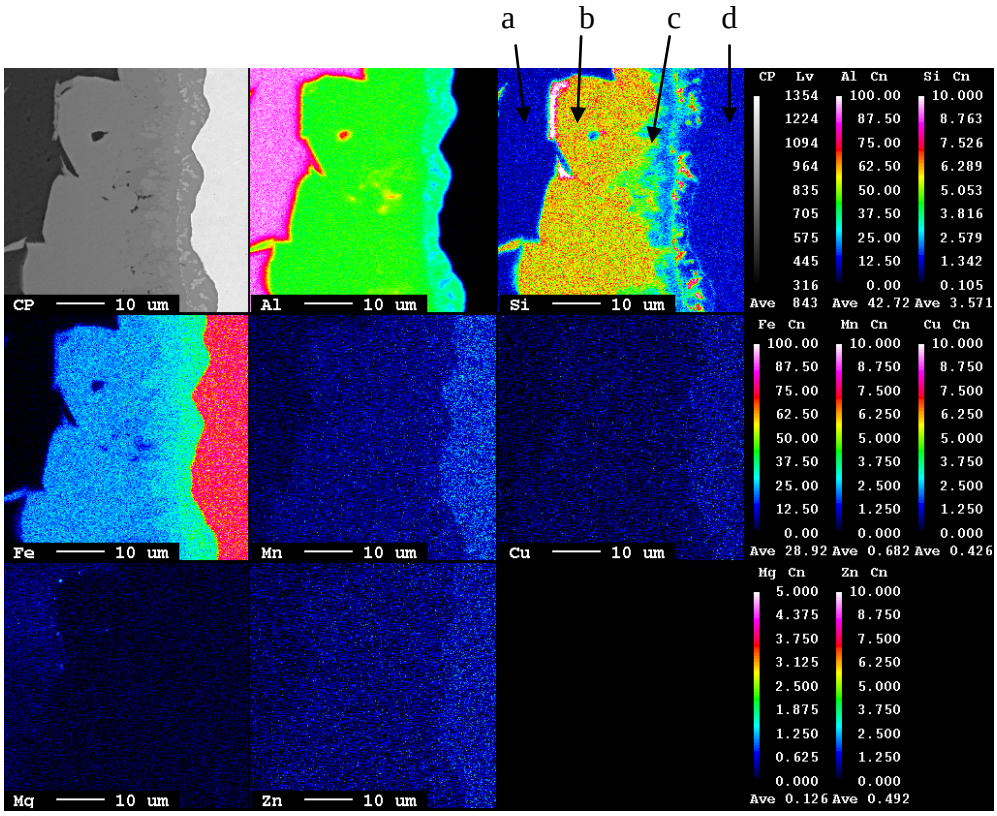

Figure 20: Map of strip hot-dipped in a fluxed commercial Al-Si 7wt% alloy at 1023K

Table 11: Point composition of coating and intermetallic layers for samples dipped in Al-Si 7wt% alloy at 1023K

Region	Al mass	Fe mass	Si mass	Mg mass	Mn mass	Cu mass	Zn mass	Total mass
a	96.348	0.504	1.43	0.239	0	0.035	0.022	98.578
a	95.048	1.041	1.751	0.208	0.012	0	0	98.06
b	55.675	30.931	10.17	0.012	0.259	0	0	97.047
b	55.53	31.449	9.652	0.005	0.143	0	0.01	96.789
b	54.212	37.915	3.35	0	0.206	0	0.063	95.746
c	55.056	37.164	2.934	0.02	0.132	0	0.081	95.387
c	49.978	41.405	2.811	0.01	0.281	0.027	0.045	94.557
c	50.546	42.09	2.137	0	0.212	0.021	0.004	95.01
d	1.041	92.02	0.695	0.034	0.591	0.023	0.048	94.452
d	0.381	93.028	0.766	0	0.439	0.077	0	94.691

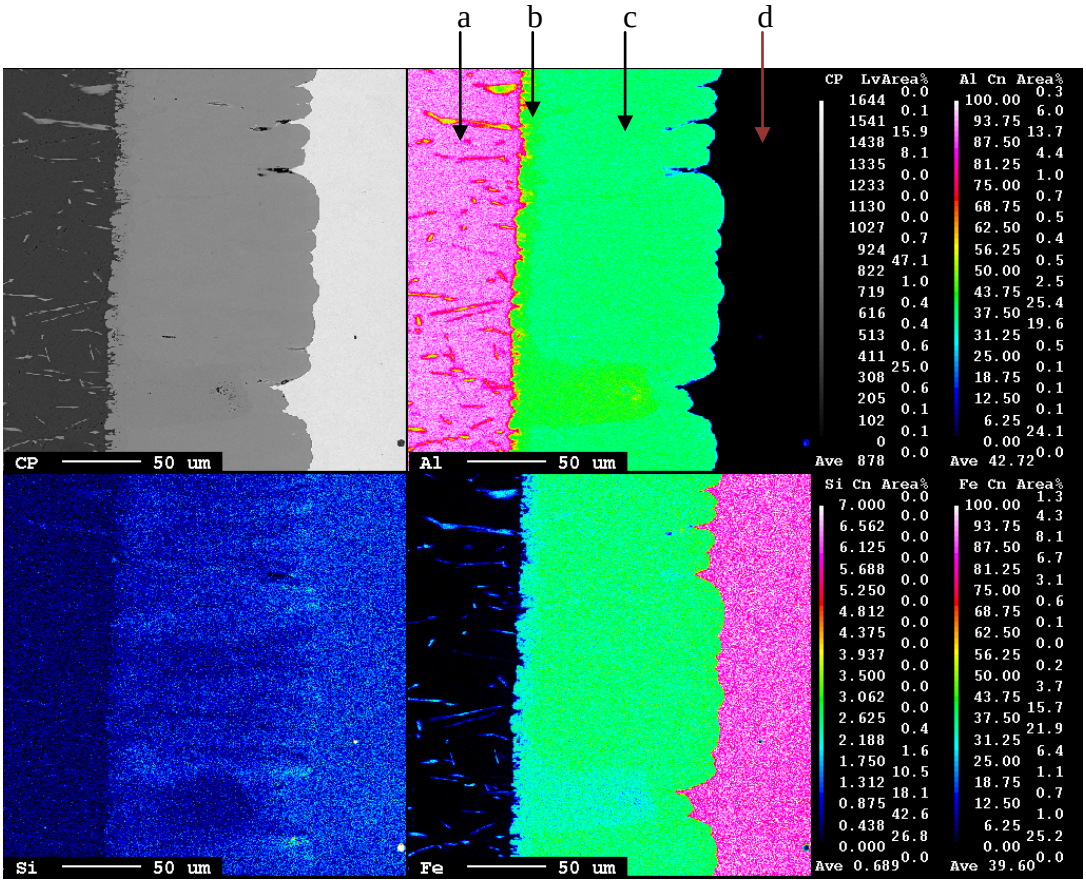

Figure 21: Map of coating and intermetallic layers for samples dipped in pure aluminium at 933K

Table 12: Point composition of coating and intermetallic layers for samples dipped in pure aluminium at 933K

region	Al mass	Fe mass	Total mass	Fe (mass %)	Al (mass%)
a	101.822	0.202	102.024	0.198	99.802
a	102.399	0.241	102.64	0.235	99.765
a	101.36	0.823	102.183	0.805	99.195
b	60.269	37.093	97.362	38.098	61.902
b	60.503	37.155	97.658	38.046	61.954
b	60.014	37.521	97.535	38.469	61.531
c	55.985	41.622	97.607	42.642	57.358
c	56.818	41.906	98.724	42.448	57.552
c	57.137	42.32	99.457	42.551	57.449
c	55.378	43.506	98.884	43.997	56.003
d	0.892	93.985	94.877	99.060	0.940
d	0.045	94.649	94.694	99.952	0.048

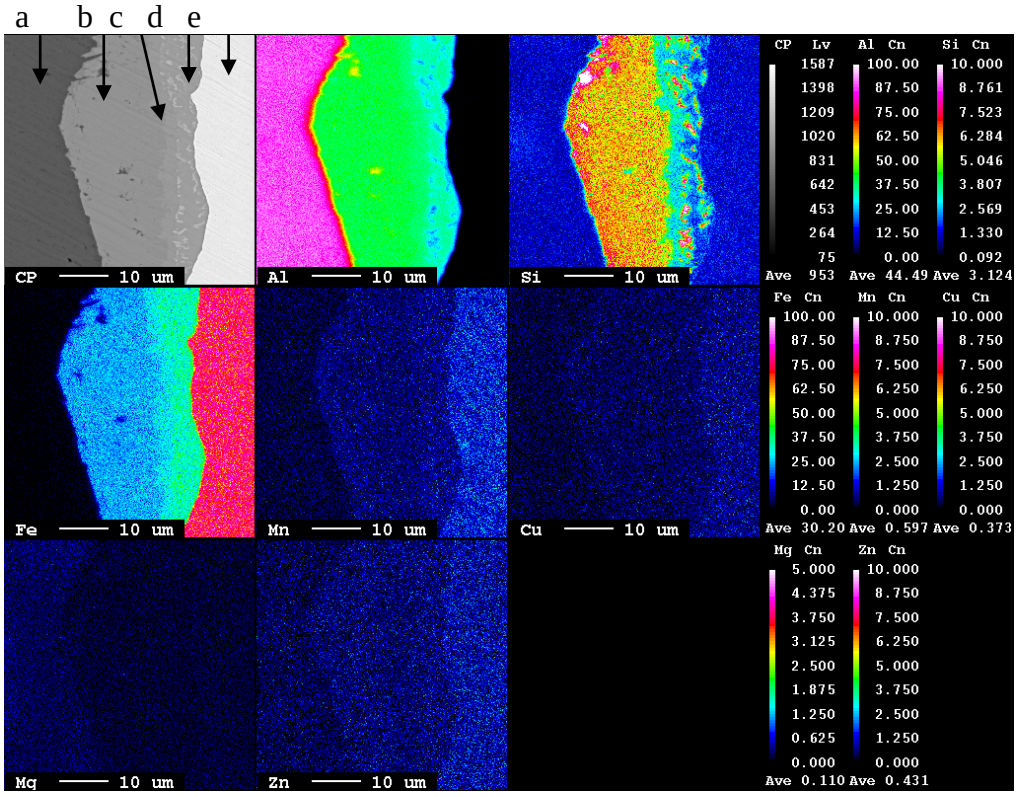

Figure 22: Map of coating and intermetallic layers for samples dipped in pure aluminium at 973K

Table 13: Point composition of coating and intermetallic layers for samples dipped in pure aluminium at 973K

region	Al mass	Fe mass	Total mass	Fe (wt %)	Al (wt %)
a	99.39	0.358	99.748	0.359	99.641
a	99.204	0.571	99.775	0.572	99.428
a	98.844	0.871	99.715	0.873	99.127
b	53.382	36.801	90.183	40.807	59.193
b	55.747	37.435	93.182	40.174	59.826
b	56.964	36.914	93.878	39.321	60.679
b	54.55	40.645	95.195	42.697	57.303
c	55.385	40.646	96.031	42.326	57.674
c	57.507	42.778	100.285	42.656	57.344
c	56.246	43.321	99.567	43.509	56.491
d	0.542	94.093	94.635	99.427	0.573
d	0.021	94.846	94.867	99.978	0.022

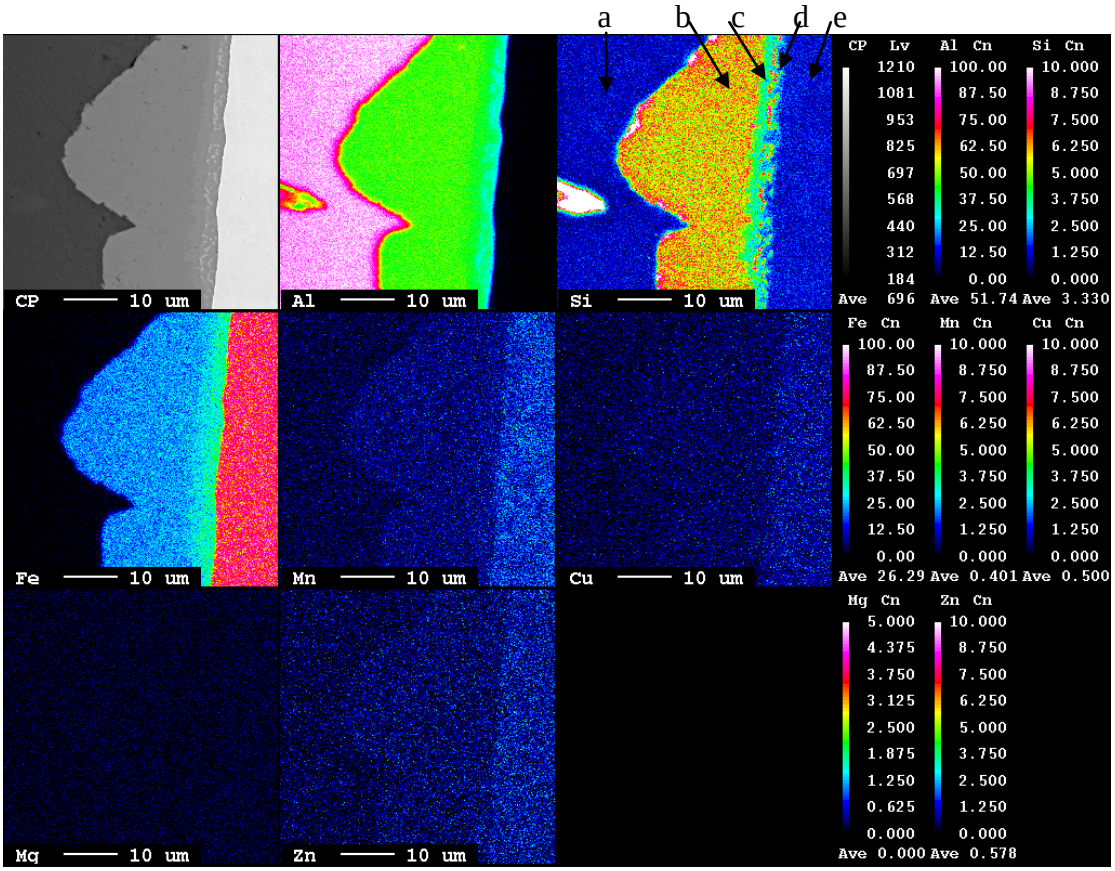

Figure 23: Map of coating and intermetallic layers for samples dipped in pure Al-Si (7wt%) at 973K

Table 14: Point composition of coating and intermetallic layers for samples dipped in pure Al-Si (7wt%) at 973K

Region	Al mass	Fe mass	Si mass	total	Al (mass %)	Fe (mass %)	Si (mass %)
a	97.179	0.699	1.338	99.216	97.947	0.705	1.349
a	96.782	0.977	1.876	99.635	97.137	0.981	1.883
b	57.552	26.276	16.291	100.119	57.484	26.245	16.272
b	58.336	25.173	15.58	99.089	58.872	25.404	15.723
b	57.294	31.719	10.789	99.802	57.408	31.782	10.810
c	52.576	41.253	4.793	98.622	53.311	41.829	4.860
d	54.929	43.392	2.009	100.33	54.748	43.249	2.002
e	0.243	95.023	0.684	95.95	0.253	99.034	0.713

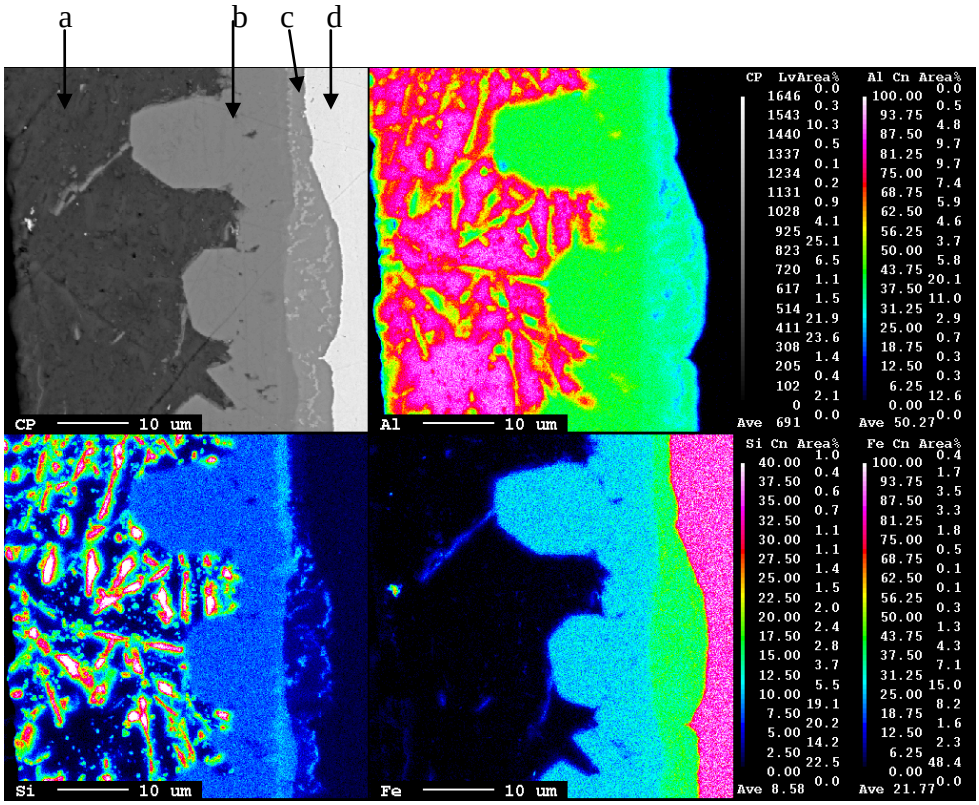

Figure 24: Map of coating and intermetallic layers for samples coated with pure Al-Si (12.5wt %) at 973K

Table 15: Point composition of coating and intermetallic layers for samples coated with pure Al-Si (12.5wt %) at 973K

Region	Al	Fe	Si	Total	Al(mass%)	Fe (mass%)	Si (mass %)
a	87.832	2.454	17.379	107.665	81.578	2.279	16.141
a	91.045	1.014	9.624	101.683	89.538	0.997	9.464
b	56.641	30.754	11.745	99.14	57.132	31.020	11.846
b	57.126	31.427	11.732	100.285	56.963	31.337	11.698
c	56.725	31.666	11.907	100.298	56.556	31.571	11.871
c	56.231	32.164	11.715	100.11	56.169	32.128	11.702
c	37.754	48.952	15.148	101.854	37.066	48.060	14.872
d	52.958	42.677	2.644	98.279	53.885	43.424	2.690
d	1.146	94.227	0.741	96.114	1.192	98.036	0.770
d	0.188	95.552	0.788	96.528	0.194	98.988	0.816

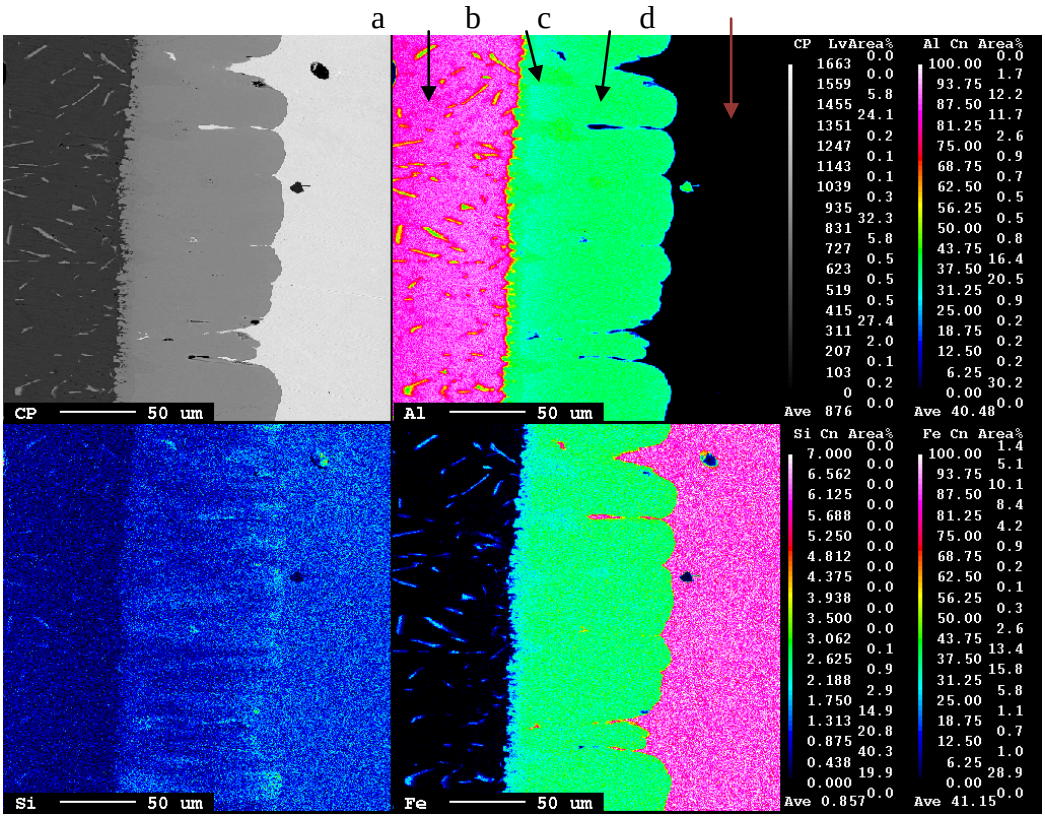

Figure 25: Map of coating and intermetallic layers for samples coated with pure Al at 973K

Table 16: Point composition of coating and intermetallic layers for samples coated with pure Al at 973K

Region	Al	Fe	total	Fe(mass%)	Al(mass%)
a	99.39	0.358	99.748	0.359	99.641
a	99.204	0.571	99.775	0.572	99.428
a	98.844	0.871	99.715	0.873	99.127
b	53.382	36.801	90.183	40.807	59.193
b	55.747	37.435	93.182	40.174	59.826
b	56.964	36.914	93.878	39.321	60.679
c	54.55	40.645	95.195	42.697	57.303
c	55.385	40.646	96.031	42.326	57.674
c	57.507	42.778	100.285	42.656	57.344
c	56.246	43.321	99.567	43.509	56.491
d	0.542	94.093	94.635	99.427	0.573
d	0.021	94.846	94.867	99.978	0.022

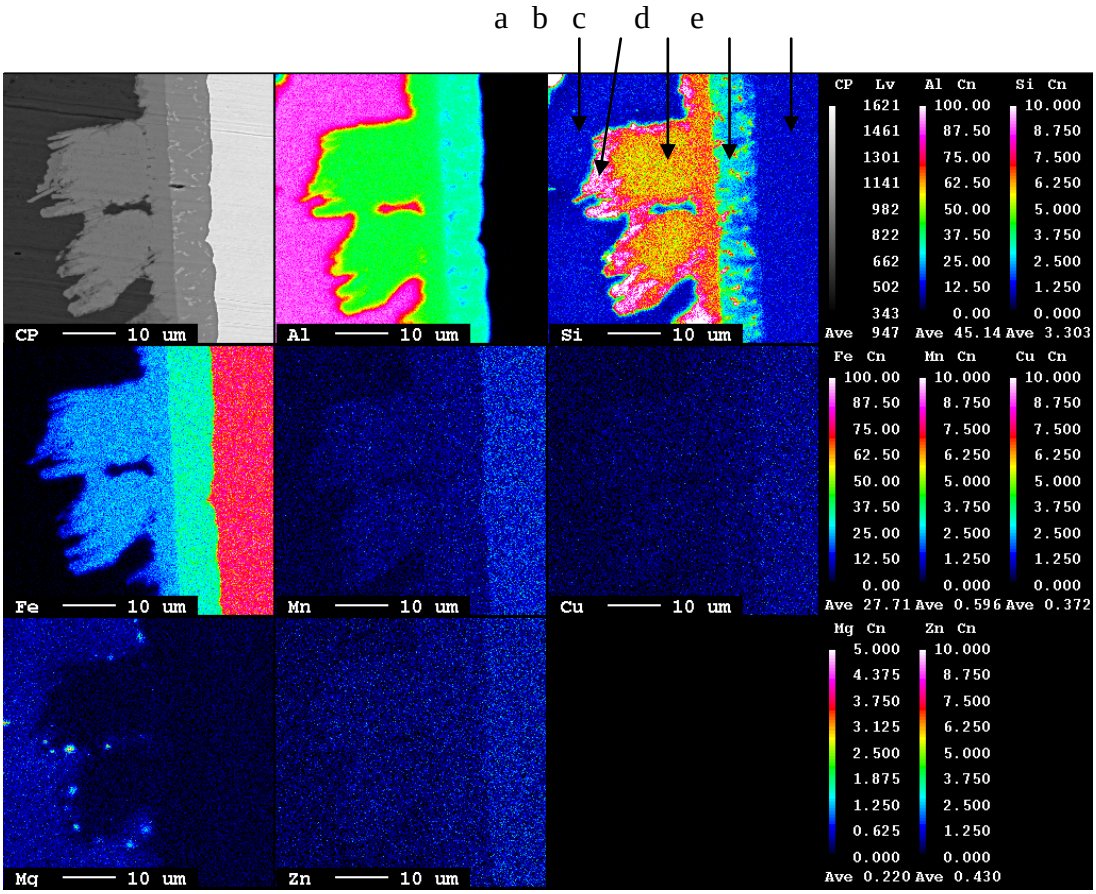

Figure 26: Map of coating and intermetallic layers for samples coated with commercial Al-Si (7wt %) at 973K

Table 17: point composition of coating and intermetallic layers for samples coated with commercial Al-Si (7wt %) at 973K

Region	Al mass	Fe mass	Si mass	Mg mass	Mn mass	Total
a	96.941	0.298	1.894	0.275	0.023	99.432
a	96.377	0.618	2.018	0.286	0.014	99.363
b	54.585	25.68	17.123	0.067	0.176	97.632
b	57.055	25.079	16.825	0.033	0.219	99.211
b	56.589	30.95	10.11	0	0.226	97.875
c	56.909	31.005	9.861	0.009	0.22	98.004
c	55.425	31.646	11.098	0.016	0.183	98.488
c	50.856	41.621	3.85	0.004	0.291	96.73
c	51.763	42.465	2.776	0.005	0.18	97.25
d	1.159	93.971	0.637	0	0.49	96.356
d	0.419	94.651	0.58	0	0.508	96.209